Journal of Geophysical Research: Atmospheres

RESEARCH ARTICLE
10.1029/2018JD028539

Special Section:
Winter INvestigation of Transport, Emissions and Reactivity (WINTER)

Top-Down Estimates of NO_x and CO Emissions From Washington, D.C.-Baltimore During the WINTER Campaign

O. E. Salmon[1], P. B. Shepson[1,2], X. Ren[3,4], H. He[4], D. L. Hall[4], R. R. Dickerson[4], B. H. Stirm[5], S. S. Brown[6,7], D. L. Fibiger[6,8,9], E. E. McDuffie[6,7,9], T. L. Campos[10], K. R. Gurney[11], and J. A. Thornton[12]

[1]Department of Chemistry, Purdue University, West Lafayette, IN, USA, [2]Department of Earth, Atmospheric, and Planetary Sciences and Purdue Climate Change Research Center, Purdue University, West Lafayette, IN, USA, [3]Air Resources Laboratory, National Oceanic and Atmospheric Administration (NOAA), College Park, MD, USA, [4]Department of Atmospheric and Oceanic Science, University of Maryland, College Park, MD, USA, [5]School of Aviation and Transportation Technology, Purdue University, West Lafayette, IN, USA, [6]Earth System Research Laboratory Chemical Sciences Division, NOAA, Boulder, CO, USA, [7]Department of Chemistry and Biochemistry, University of Colorado Boulder, Boulder, CO, USA, [8]Now at California Air Resources Board, Sacramento, CA, USA, [9]Cooperative Institute for Research in Environmental Sciences, University of Colorado Boulder, Boulder, CO, USA, [10]National Center for Atmospheric Research, Boulder, CO, USA, [11]School of Life Sciences, Arizona State University, Tempe, AZ, USA, [12]Department of Atmospheric Sciences, University of Washington, Seattle, WA, USA

Key Points:
- NEI NO_x is consistent with observations in Washington, D.C.-Baltimore, but the NEI overestimates CO emissions by a factor of 2
- Wintertime Washington, D.C.-Baltimore CO/NO_x and CO/CO_2 enhancement ratios are variable and lower than those reported by past studies
- Wintertime Washington, D.C.-Baltimore NO_x/CO_2 enhancement ratios are consistent with inventories

Supporting Information:
- Supporting Information S1

Correspondence to:
O. E. Salmon,
osalmon@purdue.edu

Citation:
Salmon, O. E., Shepson, P. B., Ren, X., He, H., Hall, D. L., Dickerson, R. R., et al (2018). Top-down estimates of NO_x and CO emissions from Washington, D.C.-Baltimore during the WINTER campaign. *Journal of Geophysical Research: Atmospheres*, *123*, 7705–7724. https://doi.org/10.1029/2018JD028539

Received 15 FEB 2018
Accepted 11 JUN 2018
Accepted article online 20 JUN 2018
Published online 23 JUL 2018

Abstract Airborne mass balance experiments were conducted around the Washington, D.C.-Baltimore area using research aircraft from Purdue University and the University of Maryland to quantify emissions of nitrogen oxides (NO_x = NO + NO_2) and carbon monoxide (CO). The airborne mass balance experiments supported the Wintertime INvestigation of Transport, Emissions, and Reactivity (WINTER) campaign, an intensive airborne study of anthropogenic emissions along the Northeastern United States in February–March 2015, and the Fluxes of Atmospheric Greenhouse Gases in Maryland project which seeks to provide best estimates of anthropogenic emissions from the Washington, D.C.-Baltimore area. Top-down emission rates of NO_x and CO estimated from the mass balance flights are compared with the Environmental Protection Agency's 2011 and 2014 National Emissions Inventory (NEI-11 and NEI-14). Inventory and observation-derived NO_x emission rates are consistent within the measurement uncertainty. Observed CO emission rates are a factor of 2 lower than reported by the NEI. The NEI's accuracy has been evaluated for decades by studies of anthropogenic emissions, yet despite continuous inventory updates, observation-inventory discrepancies persist. WINTER NO_x/CO_2 enhancement ratios are consistent with inventories, but WINTER CO/NO_x and CO/CO_2 enhancement ratios are lower than those reported by other urban summertime studies, suggesting a strong influence of CO seasonal trends and/or nationwide CO reductions. There is a need for reliable observation-based criterion pollutant emission rate measurements independent of the NEI. Such determinations could be supplied by the community's reporting of sector-specific criteria pollutant/CO_2 enhancement ratios and subsequent multiplication with currently available and forthcoming high-resolution CO_2 inventories.

1. Introduction

Nitrogen oxides (NO_x = NO + NO_2) and carbon monoxide (CO) are emitted from a variety of natural and anthropogenic sources including soil and combustion processes. NO_x and CO contribute to tropospheric ozone (O_3) production through complex reactions of peroxy radicals via hydroxyl radical oxidation of CO and volatile organic compounds (VOCs) and photolysis of NO_2. High surface-level O_3 concentrations can cause oxidative damage to crops (Van Dingenen et al., 2009). O_3 and NO_2 can irritate the human respiratory system, in part through contributions to particulate matter formation (Samet et al., 2000). CO is a toxin at sufficiently high levels (Cobb & Etzel, 1991). Because of their impacts on health, the environment, and their contribution to surface-level O_3, NO_x and CO are criteria pollutants regulated by the U.S. Environmental Protection Agency (EPA). Annual county-level emission estimates of criteria pollutants are developed by the EPA every 3 years and released as the National Emissions Inventory (NEI) to reflect the impacts of equipment innovations, new mitigation strategies, population, and the economy.

Beginning with the Clean Air Act in 1970, policies aiming to limit surface-level O_3 have targeted key sources of O_3 precursors, such as power plants and vehicles (EPA, 2004). Satellite observations have revealed significant reductions in NO_x emissions where power plant emissions dominate, such as the eastern United States, as a result of selective catalytic reduction systems (EPA, 2015a; Kim et al., 2006; Krotkov et al., 2016). Similarly, innovations in catalytic converters and NO_x after treatment technologies for gasoline- and diesel-powered vehicles have led to reductions in mobile CO and NO_x emissions (Bishop & Stedman, 2015; Dallmann & Harley, 2010; Parrish, 2006). As a result, nationwide NO_x and CO emissions have steadily decreased over the past several decades (He et al., 2013; Huang et al., 2014; Miyazaki et al., 2017; Pommier et al., 2013; Russell et al., 2012; Stavrakou et al., 2008), with indications of CO decreasing at a faster rate than NO_x (Hassler et al., 2016). While there is general consensus between inventories and observations that NO_x and CO emissions are decreasing in the United States and other developing countries (Hassler et al., 2016; Konovalov et al., 2010; Miyazaki et al., 2017; Pommier et al., 2013), discrepancies remain between observations and national inventories regarding the magnitude of current NO_x and CO emissions. Emission quantification using surface, mobile, airborne, and satellite ("top-down") measurements can be used to evaluate the accuracy of emissions inventories, that is, "bottom-up" methods (Nisbet & Weiss, 2010).

The atmospheric lifetime of CO is on the order of 1 month. NO_x, which is predominately emitted as NO and rapidly interconverts with NO_2 during the day, will react to form other oxidized nitrogen species (NO_z) including HNO_3, HONO, HO_2NO_2, peroxy nitrates, organic nitrates, and aerosol nitrate, all of which contribute to total reactive nitrogen NO_y. The interconvertible nature of NO_y species can complicate the quantification of urban NO_x emissions, and evaluation of NEI NO_x emission estimates if there is conversion of NO_x to NO_z and instrumentation is not capable of measuring NO_z species. The effective lifetime of NO_y varies by season, as it is temperature- and radiation-dependent, is highly dependent on oxidant concentrations of the hydroxyl radical (OH) and O_3, and is generally limited by dry deposition (Beirle et al., 2011; Parrish et al., 1993; Yienger et al., 1999). Transformation of NO_x to other NO_y species and depositional NO_y loss must be considered when using observational data to quantify city-wide NO_x emissions.

Previous studies usually investigated NO_y transport and reactivity in spring, summer, and fall (Chou et al., 2009; Horowitz et al., 1998; Hudman et al., 2007; Neuman et al., 2006; Singh et al., 2007; Stohl et al., 2002; Thornton et al., 2002; Zhang et al., 2016). The lack of measurements conducted during the cold season leads to greater uncertainty regarding the magnitude of wintertime NO_x emissions and the ratio of emitted NO_x relative to other combustion products. Satellite measurements not only show that urban NO_2 column densities are greater in winter than summer because of longer NO_x lifetimes (Lamsal et al., 2010; Russell et al., 2012) but also indicate that NO_x emissions are greatest in summertime as a result of soil and biomass burning emissions (Lamsal et al., 2010; Miyazaki et al., 2017). Wintertime emissions from cities could differ from other seasons due to increased residential heating, vehicles started and operated at cold temperatures, or changes in traffic patterns due to poor road conditions. These wintertime emission fluctuations could result in unique combustion product emission ratios compared to other seasons.

The Wintertime INvestigation of Transport, Emissions, and Reactivity (WINTER) was conducted along the Northeastern U.S. in February and March 2015 to investigate the lifetime, behavior, and magnitude of anthropogenic emissions during the cold season. Some of the WINTER flights overlapped in space and time with measurements of the Fluxes of Atmospheric Greenhouse Gases in Maryland project, a long-term campaign which seeks to quantify anthropogenic emissions from the Washington, D.C.-Baltimore area (D.C.-Balt).

Some field studies reported that different releases of the NEI overestimate NO_x emissions (Ahmadov et al., 2015; Anderson et al., 2014; Brioude et al., 2013; Canty et al., 2015; Castellanos et al., 2011; Hudman et al., 2007; Marr et al., 2013; Travis et al., 2016; Yu et al., 2012), while others have shown the NEI to be consistent with observations (Dallmann & Harley, 2010; Parrish, 2006). A commonly identified source of the NEI overestimation is mobile source NO_x emissions (Anderson et al., 2014; Canty et al., 2015; McDonald et al., 2012; Travis et al., 2016), which account for ~60% of nationwide NO_x in the NEI (Bishop & Stedman, 2008; EPA, 2016b). NEI mobile emissions include both "on-road" automobile emissions and "nonroad" emissions, for example, locomotives, marine, aircraft, construction, recreation, lawn/garden vehicles, and equipment (EPA, 2016b). Nonroad emissions potentially represent a significant source of uncertainty in the NEI given the relatively few studies that have characterized emission factors from the large number of nonroad vehicle/equipment types (Dallmann & Harley, 2010; Heidari & Marr, 2015).

Similarly, some studies have shown that the NEI significantly overestimates CO (Brioude et al., 2013; Fujita et al., 2012; Hudman et al., 2008; Miller et al., 2008; Parrish, 2006), while others report smaller observation-NEI discrepancies (Anderson et al., 2014; Castellanos et al., 2011; Yu et al., 2012). However, most field studies were conducted from spring throughfall (Anderson et al., 2014; Brioude et al., 2013; Canty et al., 2015; Castellanos et al., 2011; Hudman et al., 2007, 2008; Kim et al., 2016; Miller et al., 2008; Travis et al., 2016; Yu et al., 2012). The WINTER measurements over the northeastern United States allow for the evaluation of the NEI during the cold season.

The NEI is built by combining local, tribal, and state-level inventories; monitoring systems; and models (EPA, 2016b). Comparisons of top-down analyses with different releases of the NEI or with NEI estimates for different areas in the United States must be carefully considered as it is possible that NEI emission estimates are more accurate for certain sectors or certain parts of the United States. For example, power plant emissions monitored with Continuous Emissions Monitoring Systems (CEMS) are generally expected to be accurate within an uncertainty of 14% (Peischl et al., 2010; Pouliot et al., 2012). These sources can contribute significantly to regional emissions along the Ohio River Valley and the eastern United States and are responsible for ~25% of NO_x emissions nationwide (EPA, 2016b; Kim et al., 2006). Different methodologies have been developed to estimate emissions for the same sector across different years or regions. For example, the 2005 NEI relies on the MOBILE6 model to estimate automobile emissions, while the 2011 NEI uses the Motor Vehicle Emission Simulator (MOVES) model (Kota et al., 2014), except vehicle emissions for California are estimated using a California Air Resource's Board model (Kim et al., 2016). As a result, evaluations of the NEI accuracy should be interpreted as time- or region-specific.

In addition to improving future NEI estimates, sector-specific measurements of criteria pollutants, along with greenhouse gas observations, could prove helpful for building an observations-based inventory of anthropogenic emissions (Hsu et al., 2010; Warneke et al., 2007). High-resolution carbon dioxide (CO_2) inventories have been developed for the United States (Vulcan; http://vulcan.project.asu.edu) and for some U.S. cities (Hestia; http://hestia.project.asu.edu) for selected years (Gurney et al., 2009, 2012; Newman et al., 2016; Patarasuk et al., 2016). If robust NO_x/CO_2 and CO/CO_2 emission factors are determined for each contributing sector, the fuel- and activity-based Hestia CO_2 inventory can eventually be converted into nationwide NO_x and CO inventories independent of the NEI. Ratios of co-measured criteria pollutants and greenhouse gases ("emission ratios," e.g., NO_x/CO_2 and CO/CO_2) have been reported for selected cities (Brioude et al., 2013; Pollack et al., 2012; Williams et al., 2009) and could complement the development of observation-based criterion pollutant inventories. However, before a CO_2 emission inventory can be used to guide the development of new criteria pollutant inventories, appropriate criterion pollutant/greenhouse gas emission ratios must be reported from individual energy sectors, from more urban areas, and in different seasons.

To improve our understanding of wintertime emissions of reactive air pollutants, mass balance flights were conducted during WINTER using the Purdue University Airborne Laboratory for Atmospheric Research (ALAR) and the University of Maryland (UMD) experimental Cessna aircraft to quantify emission rates of NO_x and CO from D.C.-Balt. Airborne mass balance experiments have been used to quantify emissions from power plants (Ryerson et al., 1998; Trainer et al., 1995), oil and gas fields (Karion et al., 2013, 2015; Lavoie et al., 2015, 2017; Peischl et al., 2015, 2016; Pétron et al., 2014; Ren et al., 2017), and cities (Cambaliza et al., 2014, 2015; Gioli et al., 2014; Heimburger et al., 2017; Kalthoff et al., 2002; Mays et al., 2009; O'Shea et al., 2014; Salmon et al., 2017). Measurements of NO_y aboard the NCAR C-130 during WINTER are also used to provide information about NO_y partitioning downwind of D.C.-Balt. We compare our observation-derived emission rates with the 2011 and 2014 NEI (NEI-11 and NEI-14). We also report NO_x, CO, and CO_2 enhancement ratios and compare them with ratios reported from studies conducted across the United States during other seasons.

2. Methods and Data

2.1. Study Area

The D.C.-Balt urban area is centered on the cities of Washington, D.C. (38.905°N, 77.016°W) and Baltimore, MD (39.288°N, 76.617°W) and has a population of approximately 9.6 million (U.S. Census Bureau, Population Division, 2016). The Purdue and UMD experimental aircraft flights were conducted around D.C.-Balt as part of the WINTER and Fluxes of Atmospheric Greenhouse Gases in Maryland campaigns. The Appalachian Mountains lie to the west of D.C.-Balt, rural areas lie to the north and south, and the Chesapeake Bay and Atlantic Ocean lie to the east of the urban area. Similar to long-term observations of wintertime winds in

the area (Berg & Allwine, 2006), northwest winds were most commonly observed during the February and March 2015 flights. Airborne observations of urban emissions from D.C.-Balt have been previously discussed (Anderson et al., 2014; Brent et al., 2015; Castellanos et al., 2011; Hains et al., 2008; He et al., 2013, 2014, 2016; Marufu et al., 2004; Taubman et al., 2006). Observations conducted during WINTER in 2015 are compared with measurements conducted by the UMD aircraft the following February (2016) in D.C.-Balt, and in Indianapolis, IN in November to December 2014 (Heimburger et al., 2017), as part of the Indianapolis Flux Experiment (Davis et al., 2017).

2.2. Aircraft Measurements

2.2.1. Purdue Airborne Laboratory for Atmospheric Research

The Purdue ALAR was equipped with a Los Gatos Research off axis integrated cavity output spectrometer (OA-ICOS) for 1-Hz NO_2 measurements (Brent et al., 2015). The Purdue NO_2 OA-ICOS was calibrated after the WINTER campaign with an NO_2 permeation source. The measured 5-s precision for the Purdue NO_2 analyzer was ±60 pptv. A 2B Technologies Model 202 Ozone Monitor was installed in the Purdue ALAR for 0.1-Hz O_3 measurements. The Purdue O_3 analyzer was calibrated using a 2B Technologies Model 306 Ozone Calibration Source. The accuracy and detection limit for O_3 were $<$2% and 3 ppbv, respectively. Purdue's ALAR was equipped with a Picarro G2301-m CRDS for 0.5-Hz CO_2 measurements during the WINTER campaign. The Purdue CRDS was calibrated with four analytical standards from the National Institute of Standards and Technology (NIST) ranging from 359.52 to 429.68 ppmv CO_2. The measured 5-s precision for CO_2 was ±30 ppbv. Radiation (direct and diffuse) was measured by the Purdue ALAR with a LI-COR LI-200R pyranometer. The Purdue ALAR's wind system (Garman et al., 2006) and instruments for observations of other gases and aerosol during the WINTER campaign have been previously described (Salmon et al., 2017). The Purdue aircraft was used to conduct measurements in Indianapolis in November to December 2014. Methods for the Indianapolis measurements are discussed by Heimburger et al. (2017).

2.2.2. UMD Experimental Cessna

The UMD Cessna was also equipped with a Los Gatos Research OA-ICOS for 1-Hz NO_2 measurements. It was calibrated using the gas phase titration method by quantitatively converting a NIST-traceable NO standard to NO_2. The average difference between the Purdue and UMD NO_2 measurements during a 20-min intercomparison flight conducted on 19 February 2015 was 29%. Beginning on 19 February 2015, nitric oxide (NO) was measured from the UMD Cessna with a chemiluminescence NO-NO_x analyzer (Thermo Electron Corporation, Model 42) running in the NO mode. The NO analyzer was calibrated with a NIST-traceable NO standard with an accuracy of ±(3% + 50) pptv. A UV absorption O_3 analyzer (Thermo Electron Corporation, Model 49) was installed on the UMD Cessna. The O_3 analyzer was calibrated with a primary O_3 calibrator that was calibrated with a standard reference photometer at NIST. The accuracy and detection limit for the UMD O_3 measurements were $<$1% and 1 ppbv. A Picarro G2401-m cavity ringdown spectrometer for 0.5 Hz CO and CO_2 measurements was installed in the UMD Cessna. The UMD CRDS was calibrated with four NIST standards ranging from 359.52–429.68 ppmv for CO_2 and 217.00–1047.25 ppbv for CO. The measured 5-second precision for UMD CO_2 and CO measurements were ± 20 ppbv and ± 8 ppbv, respectively. Other instrumentation installed in the UMD Cessna has been discussed by He et al. (2014) and Ren et al. (2017).

2.2.3. C-130 Measurements of NO_y, CO, and CO_2

Reactive nitrogen oxides were measured using several instruments during WINTER on the C-130 aircraft. For the analysis here, NO, NO_2, and NO_y were measured with a NOAA custom-built CRDS. NO_2 was measured by direct absorption at 405 nm (Fuchs et al., 2009) and was calibrated throughout the campaign by measurement of NO_2 converted from known amounts of O_3 in excess NO (Washenfelder et al., 2011). The stated accuracy and 1σ 1-s precision of the NOAA CRDS instrument is 3% and $<$30 pptv for NO_2 (Wild et al., 2014) but was $<$8% and 114 pptv, respectively, on C-130 research flights 1 and 2 (3 and 6 February 2015) due to an inlet zero issue. NO_y was thermally converted in a quartz heater (650°C) and measured as NO_2 in a separate channel after chemical conversion of NO to NO_2 via excess O_3 (Wild et al., 2014). The NO_y channel is calibrated using the same method as the NO_2 channel and had an accuracy of 12% and 1σ 1-s precision of 190 pptv for the C-130 flights considered here.

Carbon monoxide was measured by a commercial Aero-Laser AL-5002 VUV resonance fluorescence instrument having a 1.5-ppbv precision (1σ 1-s) and 0.5-Hz frequency response. A Picarro G2311-f CRDS instrument quantified CO_2 dry mole fraction with a 1σ 0.2-s precision of 250 ppbv, with a 2-Hz frequency response.

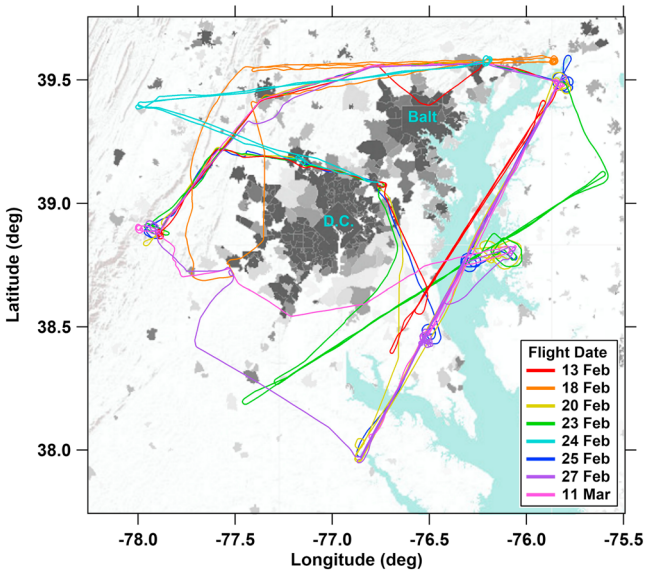

Figure 1. Mass balance flight paths conducted around D.C.-Balt during Wintertime INvestigation of Transport, Emissions, and Reactivity. Northwest winds were typically observed during D.C.-Balt mass balance flights, except for 18 February 2015 (orange) and 24 February (light blue) when winds were from the south. Map source: Esri, U.S. Geological Survey, National Oceanic and Atmospheric Administration, 2010 U.S. Census. Population density (shown in gray) is distributed by the U.S. Census Bureau's populated place definitions.

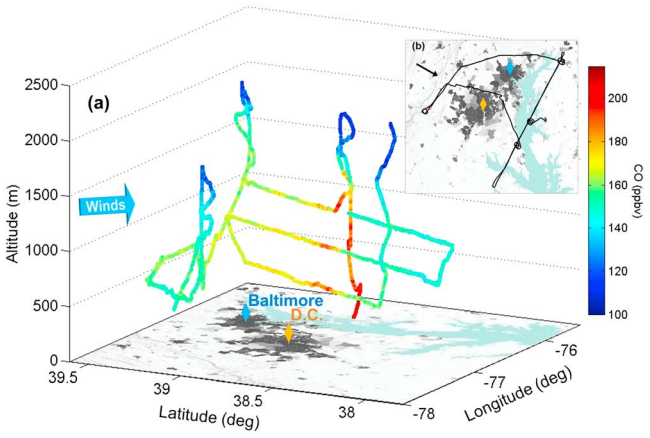

Figure 2. (a) Three-dimensional view of the mass balance flight conducted around D.C.-Balt on 25 February 2015. The flight path is colored by CO mixing ratio. The experiment began with a vertical profile upwind of the urban area, followed by an upwind transect. Three transects were then conducted downwind of the city. Three additional vertical profiles were conducted downwind of the study area to characterize vertical mixing. Segments traveling to and from the home airport have been removed from (a) for clarity. (b) The two-dimensional top view of the entire flight path. Map source: Esri, U.S. Geological Survey, National Oceanic and Atmospheric Administration, 2010 U.S. Census. Population density (shown in gray) is distributed by the U.S. Census Bureau's populated place definitions.

2.3. Airborne Mass Balance Experiment

Emission rates from D.C.-Balt were quantified from airborne mass balance measurements conducted by the UMD and Purdue aircraft on the weekdays: 13, 18, 19, 20, 23, 24, 25, and 27 February and 11 March 2015. Flight paths are shown in Figure 1 (Table S1 in the supporting information is a flight log detailing all the flights discussed in this paper). Mass balance measurements conducted on 19 February 2015 were used to quantify emissions from an energy generating facility in Maryland. Mass balance experiments were conducted during afternoon hours when boundary layer conditions are most constant relative to other times of the day (Stull, 1988). Flights initiated at approximately noon and ended in late afternoon before boundary layer decay began (Acevedo & Fitzjarrald, 2001; Lothon et al., 2014). Figure 2a shows an example three-dimensional mass balance flight path colored by CO mixing ratio for 25 February 2015, and the inset (Figure 2b) shows the two-dimensional top view of the flight path. Flights typically began with a vertical profile conducted upwind of the study area to estimate boundary layer height, followed by an upwind transect to measure inflow mixing ratios. Then, typically three downwind transects were conducted approximately equally spaced throughout the boundary layer. At some point during the downwind transects, an additional vertical profile (s) was (were) conducted downwind of the study area, usually within the urban plume, to characterize vertical mixing and identify boundary layer evolution throughout the duration of the flight.

2.4. Calculation of NO_x

Only NO_2 was measured during the Purdue ALAR mass balance flights, while NO and NO_2 were both measured by the UMD Cessna (except for one UMD flight on 13 February 2015 when only NO_2 was measured). For mass balance days when NO_x cannot be directly calculated from measurements, NO_x is defined as the sum of calculated steady state NO (NO_{ss}) and measured NO_2 (Leighton, 1961). The step-by-step calculation of NO_{ss} using airborne measurements of NO_2, O_3, and calculated NO_2 photolysis rates is discussed in detail in Text S1 and Figures S1 and S2 in the supporting information, along with a discussion of associated uncertainties.

2.5. Background Determination

To determine the urban enhancement in CO and NO_x, background values ($C_{bg,i}$; C is CO or NO_x) are subtracted from the elevated downwind mole fractions of CO and NO_x ($C_{dw,i}$). Point-by-point urban enhancements in NO_x and CO are identified as $X_{NOx,i}$ and $X_{CO,i}$, as in equation (1):

$$X_{C,i} = C_{dw,i} - C_{bg,i} \quad (1)$$

Background mole fractions are defined by fitting an ordinary least squares linear regression to the rural area-influenced mole fractions on either side of the urban plume (Cambaliza et al., 2014, 2015; Heimburger et al., 2017; Karion et al., 2015; Salmon et al., 2017), analogous to defining the baseline of a chromatographic peak. We define the transition from rural- to urban-influenced air as the point when the downwind NO_x and CO mole fractions are greater than the background plus 3 times the observed standard deviation of the background, which is defined as the standard deviation in the

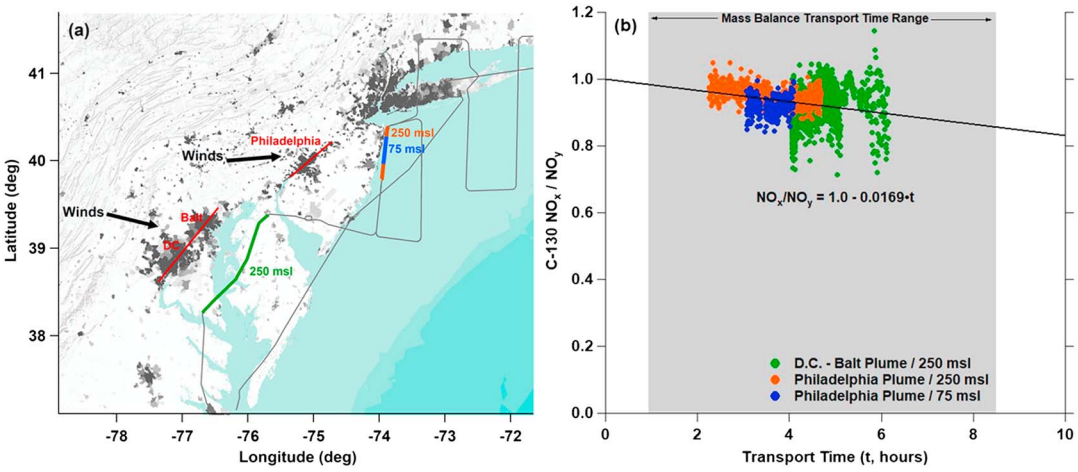

Figure 3. (a) C-130 flight path on 3 February 2015 flown downwind of D.C.-Balt and Philadelphia. The D.C.-Balt and Philadelphia "emission areas" are indicated by the red trace. Transport times are defined as the time between emission from D.C.-Balt or Philadelphia (red trace) and sampling downwind by the C-130 (transect altitudes are reported in meters above sea level). Map source: Esri, U.S. Geological Survey, National Oceanic and Atmospheric Administration, 2010 U.S. Census. Population density (shown in gray) is distributed by the U.S. Census Bureau's populated place definitions. (b) The ratio of NO_x/NO_y sampled by the C-130 within the isolated plumes indicated in (a) plotted as a function of transport time between emission and sampling.

atmospheric species along the upwind transect. For the regression analysis, the aircraft's location along the downwind transect is the independent variable and the dependent variable is the rural-influenced NO_x or CO mole fractions. This method for background determination has been evaluated by Heimburger et al. (2017). The D.C.-Balt NO_x and CO plumes with defined backgrounds are provided in Figures S3 and S4, respectively.

2.6. Transformations of NO_x

Transformations of NO_x to NO_z must be accounted for in the D.C.-Balt mass balance analysis for meaningful reporting of city-wide NO_x emissions and comparison to the NEI. The NEI reports NO_x emissions from the source. After being emitted, NO_x can react to form NO_z, for example, HNO_3, HO_2NO_2, peroxyacyl nitrates, organic nitrates ($RONO_2$), and aerosol nitrate. We assume that the NO_y molecules contributing to the observed urban enhancement downwind of the study area were all initially emitted as NO_x, and, because of the short atmospheric processing time between emission and measurement (average: 2.8 hr), NO_y removal is relatively small (~11%, calculation in Text S2). During the day, the downwind ratio of NO_x/NO_y is dependent on NO_y photochemical reaction and deposition rates and theoretically varies with the age of the air parcel since emission.

The relationship between air parcel transport time and NO_x/NO_y was determined for three isolated urban plumes sampled by the C-130 aircraft (flight path in Figure 3a) during afternoon hours (14:45–17:15 EST). The measured NO_x/NO_y ratios within the three urban plumes are plotted as a function of transport time (t) in Figure 3b. Transport times were determined using the National Oceanic and Atmospheric Administration Air Resources Laboratory's Hybrid Single-Particle Lagrangian Integrated Trajectory model (Stein et al., 2015), which was defined as the time lapse between when the air parcel passed over the D.C-Balt or Philadelphia area and when the air parcel was sampled. For this analysis, the D.C.-Balt area was defined as the line intersecting the geographical coordinates of Washington, D.C. and Baltimore, MD, and the Philadelphia area was defined as the best fit line of the geographical coordinates of Trenton, NJ; Philadelphia, PA; and Wilmington, DE (red traces in Figure 3a).

Hybrid Single-Particle Lagrangian Integrated Trajectory-calculated transport times (t) can be used as inputs for equation (2) to calculate the NO_x/NO_y ratios downwind of D.C.-Balt during the mass balance flights (which did not have NO_z measurements). To account for transformations of NO_x to NO_z species, the urban NO_x enhancements ($X_{NOx,i}$; equation (1)) were divided by the calculated NO_x/NO_y (equation (2)) to give the calculated NO_y enhancements ($X_{NOy^*,i}$; where the asterisk indicates "calculated"), as in equation (3).

Table 1
Distribution of NEI-11 D.C.-Balt NO_x and CO Emissions by Sector

Source sector	NO_x		CO	
	Feb	Mar	Feb	Mar
On-road	49.4%	52.1%	49.4%	48.9%
Nonroad	12.1%	15.3%	21.5%	34.6%
Point	16.0%	16.7%	4.1%	4.4%
Nonpoint	17.3%	11.1%	15.3%	10.3%
Marine	3.5%	3.9%	0.1%	0.1%
Fire	1.0%	0.1%	9.5%	1.2%
Biogenic	0.6%	0.8%	0.2%	0.4%

$$\left(NO_x/NO_y\right)_i = 1.0 - 0.0169 \cdot t \quad (2)$$

$$X_{NOy*,i} = \frac{X_{NOx,i}}{\left(NO_x/NO_y\right)_i} \quad (3)$$

Uncertainties and assumptions associated with the calculation of NO_y, including the temporal variability of NO_x/NO_y (Ren et al., 2006), NO_y removal via dry deposition(Sickles & Shadwick, 2007; Zhang et al., 2012), and the vertical gradient of NO_x/NO_y within the boundary layer, are discussed in Text S2 and Figure S5.

2.7. Emission Rate Calculation

To quantify the total emission rate of NO_{y*} and CO from the D.C.-Balt area, fluxes, $F_{C,\,i}$, of the scalar, C (NO_{y*} or CO), are calculated at each downwind sampling point according to equation (4).

$$F_{C,i} = U_{\perp,\,i} \cdot X_{C,i} \quad (4)$$

In equation (4), the urban enhancement $X_{C,\,i}$ (mol m^{-3}) in CO or NO_{y*} is multiplied by the component of the wind speed (10-s average) perpendicular to the downwind flight track, $U_{\perp,\,i}$ (m s^{-1}), to yield a flux, $F_{C,\,i}$ (mol m^{-2} s^{-1}), across an imaginary vertical plane downwind of the source region. An expanded form of equation (4) is provided in Text S3.

The flux values calculated at each downwind sampling point, $F_{C,\,i}$, are interpolated/extrapolated to create a two-dimensional x-z plane, or matrix (M_C) of downwind CO or NO_{y*} fluxes (Heimburger et al., 2017). The matrix extends from the surface to the top of the boundary layer and only extends horizontally to include urban-influenced air (section 2.5). The average boundary layer height during the WINTER D.C.-Balt mass balance flights was 1,200 m (Table S1). Determination of boundary layer height (z_i) from vertical profiles is defined by the greatest increase in potential temperature with altitude (Bonin et al., 2018; Cambaliza et al., 2014). The citywide emission rate, ER_C (mol s^{-1}), is calculated by integrating the pixels of the flux matrix, M_C, across the horizontal bounds of the city, and vertically from the surface to the top of the boundary layer according to equation (5):

$$ER_C = \int_0^{z_i}\int_{-x}^{+x} M_C\,dx\,dz \quad (5)$$

Uncertainties associated with the CO and NO_{y*} mass balance rate calculation are discussed in Text S3 and Table S2.

2.8. Emission Inventories

We conduct a 1:1 comparison of our top-down D.C.-Balt NO_{y*} (hereon referred to as NO_x) and CO emissions estimates to version 2 of the NEI-11 and version 1 of the NEI-14 (EPA, 2015b; EPA, 2016b). NEI-11 and NEI-14 annual county NO_x and CO emissions are temporally allocated by month and projected forward in time to 2015 with version 6.2 of the EPA's 2011 Emissions Modeling Platform (EPA, 2015c). For reference, the sector breakdown of NEI-11 D.C.-Balt NO_x and CO emissions is provided in Table 1 (EPA, 2015c). Inventory CO_2 estimates for the D.C.-Balt study area are determined from the Vulcan 2002 fossil fuel CO_2 emission inventory and scaled by population growth to 2015 (version 2.2; http://vulcan.project.asu.edu/) (Gurney et al., 2009).

We assume that the co-emitted combustion products CO_2, CO, and NO_x follow a similar diurnal emission profile. The temporal structure of Hestia's 2014 Baltimore CO_2 data product (http://hestia.project.asu.edu/) is used to temporally allocate the D.C.-Balt Vulcan CO_2 and NEI-11 and NEI-14 monthly NO_x and CO emissions estimates into hourly emission rates. We opt to use the Hestia Baltimore emission trends because Hestia represents fossil fuel combustion emissions within our study area which are available at hourly resolution. WINTER 2015 CO and NO_x emissions were also calculated from Sparse Matrix Operator Kernel Emissions (SMOKE) outputs based on the NEI-11, as described by Anderson et al. (2014). The SMOKE analysis predicted slightly higher afternoon CO (1,500 ± 500 mol s^{-1}) and NO_x (170 ± 20 mol s^{-1}) emission rates compared to the interpolated, forward-projected, temporally allocated NEI CO (~1,100 mol s^{-1}) and NO_x (~115 mol s^{-1})

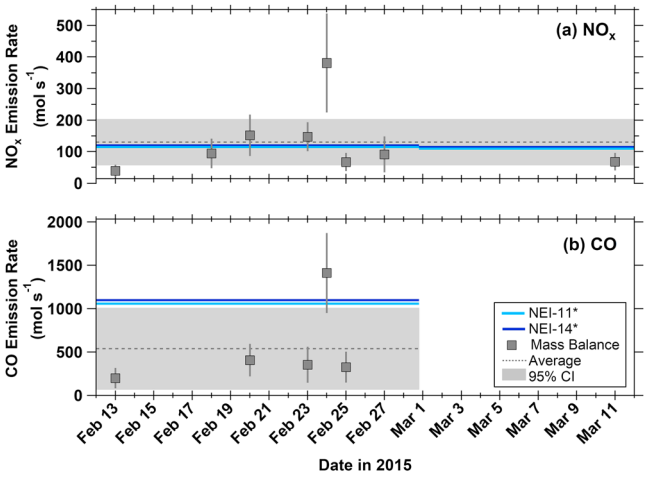

Figure 4. Time series of D.C.-Balt top-down emission rate estimates for (a) NO_x and (b) CO calculated (equations (4) and (5)) using measurements made during mass balance flights. NEI-11* and NEI-14* NO_x and CO emissions estimates indicate NEI emissions forward-projected to 2015.

emission estimates. A step-by-step explanation of the scaling/temporal allocations conducted on the D.C.-Balt emission inventories, as well as discussion of the SMOKE analysis (EPA, 2014a, 2014b; Goldberg et al., 2015, 2016; Houyoux & Vukovich, 1999; Kota et al., 2012; Vinciguerra et al., 2017), is provided in Text S4 and Figures S6 and S7.

Emissions from an energy generating facility in Maryland were estimated from measurements made downwind of the facility on 19 February 2015 and were compared with the EPA's CEMS data, which reports hourly, facility-level NO_x and CO_2 emissions. NEI and CEMS NO_x are converted to moles assuming all the NO_x is NO_2 according to the EPA definition (molar mass: 46 g mol^{-1}) because NO_2 is an EPA criteria pollutant. NEI CO emissions are converted to moles using CO molar mass (28 g mol^{-1}).

3. Results and Discussion

3.1. Emission Rate Comparison: Top-Down Versus Bottom-Up

3.1.1. NO_x

Figure 4a is a time series of NO_x emission rates calculated from the mass balance flight measurements (corresponding values are listed in Table S3). NO_x emission rates are calculated from NO_y enhancements (section 2.7) but are reported as "NO_x" for consistency with the NEI. The average top-down afternoon NO_x emission rate was 130 mol s^{-1}, with a 95% confidence interval (CI) for the mean ($\bar{x} \pm ts/\sqrt{N}$; $s = \pm 110$ mol s^{-1}; $t = 1.895$; $N = 8$) ranging from 60 to 200 mol s^{-1}. The NEI-11 (NEI-14) February and March 2015 afternoon NO_x emission rates are 115 (120) and 110 (115) mol s^{-1}, respectively. While the observations are consistent with the NEI, our city-scale measurements do not allow us to evaluate how accurately the NEI estimate emissions from the component source sectors. Past studies have found that total NEI NO_x emissions agree with observations, but observed sector contributions were inconsistent with the NEI's distribution of emissions (Dallmann & Harley, 2010).

As can be noted from Figure 4, the 24 February emission rates were higher relative to the other flight days. Excluding the 24 February NO_x emission rate from the analysis results in an average D.C.-Balt NO_x emission rate of 95 mol s^{-1}, and the 95% CI ranges from 65 to 125 mol s^{-1}. We opt to include the 24 February data point in our analysis because the NO_x emission rate on this day is not a statistical outlier, and the 95% CI in both scenarios are consistent with NEI NO_x emissions. According to the CEMS data, NO_x (and CO_2) emissions from energy production were highest on the 20 February 2015 flight day, followed by 24 February 2014. Daily CEMS NO_x (and CO_2) emissions on 24 February were within 1σ of the average of all the flight days. Relative to the other flight days, 24 February was the second-coldest flight day (20 February was the coldest), but again the average daily temperature was not significantly lower than the flight days. Other emission sources might be responsible for the anomalously high 24 February NO_x emissions, such as mobile (on road and/or nonroad) emissions (Table 1). However, 24 February 2015 was a Tuesday, not a holiday, and it had not snowed or rained on this day. We do not expect significant changes in mobile on road or nonroad vehicles emissions.

The 24 February flight day (Figure 4) was unique in that a low-pressure system was moving into the study area. Barometric pressure decreased steadily throughout the day, whereas barometric pressure was relatively constant or increased throughout the afternoons of the other study days. Clocking (counterclockwise direction) winds, which are associated with low-pressure systems, were present in the morning (https://www.wunderground.com/history/airport/KDCA/2015/2/24/DailyHistory.html). The low, circling winds in the morning, aided by the Appalachian Mountains which lie to the west, and the Atlantic Ocean which is east of D.C.-Balt, possibly acted to trap emissions within the study area. Wind speeds began to increase around 12:00 local time and possibly helped flush the trapped emissions out of the study area. Airborne measurements downwind of D.C.-Balt on 24 February 2015 were conducted between approximately 12:30–13:45 and possibly sampled accumulated emissions resulting in an anomalously high NO_x emission rate this day.

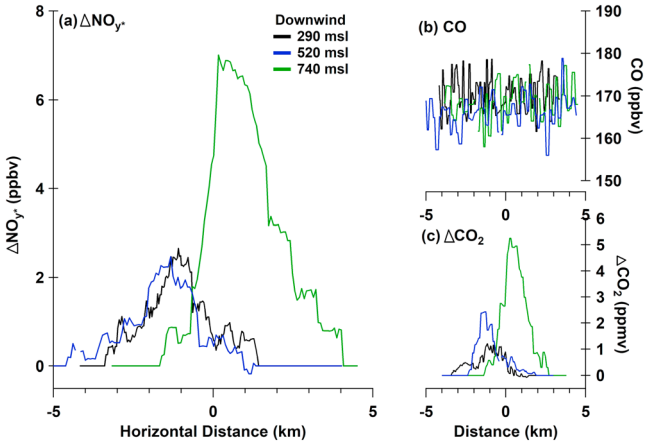

Figure 5. Plume profiles of (a) ΔNO_{y^*}, (b) CO, and (c) ΔCO_2 sampled downwind of the chalk point generating station in Maryland on 19 February 2015. The triangle indicates that the plumes shown are background-subtracted enhancements.

The NO_x mass balance error propagation (Text S3 and Table S2) resulted in an average uncertainty of ±45% for the individual top-down NO_x emission rates. This is similar to the uncertainty estimate for the mass balance approach for single determinations, reported by Cambaliza et al. (2014). A detailed description of the uncertainty analysis is provided in Text S3 and Table S2. In addition to the uncertainty in the measurements of pressure, temperature, winds, and NO_x mole fraction, the analysis accounts for the uncertainty associated with calculating NO_{y^*} from the NO_x enhancements, which is defined by (1) the uncertainty in calculated NO_x/NO_y ratios (~6%) and (2) NO_y removal via dry deposition (~11%). For the flight days in which NO_x was calculated as the sum of measured NO_2 and calculated NO_{ss}, the uncertainty associated with the J_{NO2}-Irradiance relationship in equation (S2) (~6%) and the photochemical stationary state assumption (~15%) are also propagated.

NO_x emissions from the Chalk Point Generating Station, a 2,600-MW energy generating facility fueled primarily by coal, as well as oil and natural gas, in Eagle Harbor, Maryland (38.5444, −76.6861), were quantified from measurements collected during a mass balance flight on 19 February 2015 between approximately 15:00 and 17:00 EST by the UMD aircraft (Figure 5). Total urban area NO_x emission rates from D.C.-Balt were not quantified for this flight because background mole fractions sampled at the edges of the downwind transects were variable. Relatively constant background NO_x mole fractions were, however, definable on either side of the power plant plume, likely due to the close proximity of the downwind transects to the facility (average transport time between emission and sampling was 30 min).

The emission rate of NO_x from the energy generating facility was calculated to be 6.2 (±2.1) mol s^{-1}. The NO_x emission rate reported by the CEMS for the facility was 9.3 (±1.3) mol s^{-1} over the 3-hr period when the downwind transects were conducted. According to CEMS data, the energy output of the power plant increased by 200 MW h^{-1} during the experiment. The magnitude of the CEMS hourly reported NO_x and CO_2 emissions reflect this increase in energy output. The CEMS-reported emission rate and the NO_x emission rate calculated from the mass balance flight are not statistically significantly different at the 95% confidence level. The facility's CO_2 emission rate of 3430 (±740) mol s^{-1}, quantified from the mass balance measurements, was slightly lower than the CEMS-reported average CO_2 emission rate of 5,100 mol s^{-1} (±710). Some quantitative studies of power plant emissions have found ambient observations to be consistent with CEMS data within the CEMS's specified accuracy of 14% (Peischl et al., 2010), while inconsistencies between CEMS and observations have also been reported (Placet et al., 2000). NO_x/CO_2 emission ratios from the energy generating facility are discussed in section 3.2.3. An enhancement in CO mole fraction was not detectable downwind of the facility (Figure 5b). Power plant CO emissions have been reported to be temporally variable and dependent on type of fossil fuel used and plant operating conditions (Nicks Jr et al., 2003; Peischl et al., 2010).

3.1.2. CO

Figure 4b shows the CO emission rates calculated from measurements made during the UMD mass balance flights (corresponding values are listed in Table S3). The average afternoon CO emission rate calculated from UMD's airborne measurements is 540 mol s^{-1}, and the 95% CI ($\bar{x}\pm ts/\sqrt{N}$; s = ±490 mol s^{-1}; t = 2.132; N = 5) ranges from 70 to 1010 mol s^{-1}. The large 95% CI for CO is strongly influenced by the high emission rate of CO from D.C.-Balt on 24 February 2015 (discussed below). High emissions of NO_x were also observed that day. The variability in CO emission rates in Figure 4b could indicate that day-to-day D.C.-Balt CO emissions can be highly variable or reflect the mass balance emission rate uncertainty. The individual flight day CO emission rate uncertainty (Text S3), indicated by the error bars in Figure 4b, was calculated to be ±50% on average. The NEI-11 and NEI-14 February 2015 afternoon CO emission rate estimates are 1,060 and 1,100 mol s^{-1}, respectively, a factor of ~2.0 greater than the average top-down CO emission rate estimate. Our determination of the CO emission rate is statistically significantly different from the stated NEI values (however, the NEI does not report uncertainties). Miller et al. (2008) found the NEI-99 overestimated nationwide CO emissions

by a factor of 2 and 3 in spring and summer, respectively. Similarly, Brioude et al. (2013) report that posterior CO emissions from the Los Angeles Basin constrained by observations during CalNex (May–June 2010) were a factor of 2 lower than the 2005 version of the NEI, which was used as the prior.

The calculated CO emission rate on 24 February 2015, 1,400 (±460) mol s^{-1}, was the highest observed in D.C.-Balt during WINTER. It is the only CO emission rate estimate that is consistent with the NEI (~1,100 mol CO s^{-1}). The 24 February CO emission rate is also an outlier (even when accounting for the CO mass balance measurement uncertainty). The outlier definition assumed here is a number more than 1.5 times the interquartile range above the third quartile (or below the first quartile). Excluding the 24 February CO emission rate from the analysis results in an average D.C.-Balt CO emission rate of 320 mol s^{-1}, and the 95% CI ranges from 230 to 415 mol s^{-1}. We opt to include the 24 February observations in this analysis because the NO_x emission rate for this day is not an outlier when the 24 February 41% NO_x mass balance measurement uncertainty (Table S2) is considered. Furthermore, not including the 24 February observations results in an average D.C.-Balt CO emission rate that is a factor of 3 lower than the NEI, whereas including it leads to a factor of two difference between the inventory and observations. In either scenario the observed CO emissions are significantly lower than the NEI. As discussed in section 3.1.1, airborne measurements downwind of D.C.-Balt on 24 February 2015 possibly reflect a component of accumulated morning emissions, which were flushed out of the study area by strong southerly winds in the afternoon, resulting in anomalously high NO_x and CO emission rates.

According to the EPA Emissions Modeling Platform, on-road mobile sources are the dominant contributors to D.C.-Balt CO emissions (Table 1). This points us to consider mobile on-road emissions as an obvious potential source of the discrepancy between the NEI and observations. Additionally, the nonroad sector, the second largest contributor to the area's CO emissions, accounts for 21.5% and 34.6% of D.C.-Balt's CO emissions for February and March, respectively (Table 1). It is the largest (February–March) change in NO_x or CO sector contributions during the study months (Table 1). This change in sector contributions could be indicative of a transition in the vehicles/equipment contributing to the study area's emissions. For example, the increase in nonroad contributions could reflect an increase in lawn/garden or construction emissions as weather becomes milder. While some studies have found the NEI nonroad emissions to be consistent with observed estimates (Kim et al., 2016), several studies have noted the uncertainty in NEI nonroad emission estimates since many types of vehicles/equipment fall into the category (e.g., construction, agriculture, lawn/garden, and recreation vehicles and equipment) and have unique emission profiles (Dallmann & Harley, 2010; Heidari & Marr, 2015). For example, Heidari and Marr (2015) showed some construction vehicles emitted up to a factor of 100 lower than predicted by the NEI, while observed emissions from other types of construction vehicles were consistent with the NEI. The temporally abrupt period over which this increase in nonroad sector contributions occurs possibly points to an additional component of uncertainty in the NEI's estimation of nonroad CO emissions. While on-road emissions account for approximately half of the D.C.-Balt CO emissions in February and March (Table 1), the nonroad sector represents a possibly significant component of the factor of 2 discrepancy between the NEI and WINTER observations.

3.2. Enhancement Ratios

Here we report enhancement ratios of CO/NO_x, NO_x/CO_2, and CO/CO_2 ("enhancement" indicates that ratios are determined for background-subtracted urban emissions). Enhancement ratios can serve as indicators of temporal emission trends (Bishop & Stedman, 2015; Dallmann & Harley, 2010; Hassler et al., 2016; Parrish et al., 2002) and can be compared across cities, energy sectors, and fuel types (Anderson et al., 2014; Peischl et al., 2010; Williams et al., 2009). Robust NO_x/CO_2 and CO/CO_2 emission factors for contributing sectors would allow the Hestia, Vulcan, or other CO_2 inventories to eventually be utilized to enable production of nationwide NO_x and CO inventories that are independent of the NEI. This approach could then result in more reliable NO_x and CO emission inventories, as long as these sector-specific emission factors were regularly updated.

Enhancement ratios are defined as the correlation slope between background-subtracted urban enhancements of CO, NO_y, and CO_2 (Anderson et al., 2014; Brioude et al., 2013; Hassler et al., 2016; Parrish, 2006; Pollack et al., 2012; Williams et al., 2009). Because CO and CO_2 are relatively long-lived, the mole fractions measured downwind of D.C.-Balt could contain components related to long range transport. It is thus

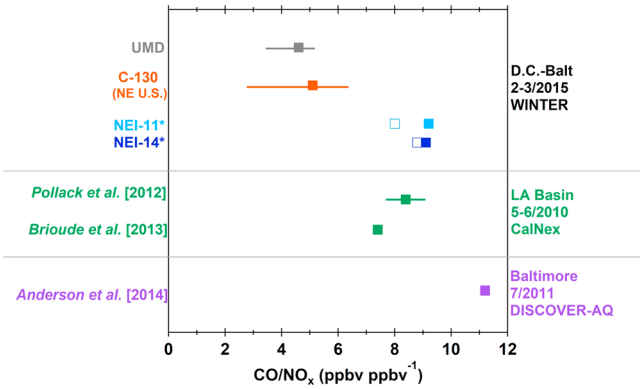

Figure 6. CO/NO_x enhancement ratios calculated from the University of Maryland aircraft and C-130 observations are compared with the National Emissions Inventory (NEI) and other urban studies. The markers indicate average enhancement ratios (solid bars identify the range of ratios observed on individual flight days). The unfilled and filled NEI markers indicate original NEI emissions and NEI emissions forward-projected to 2015, respectively.

necessary to determine the correlation of background-subtracted data (section 2.5). The enhancement ratios CO/NO_x and NO_x/CO_2 are reported with the nomenclature "NO_x" for consistency with the NEI but are calculated using background-subtracted NO_y to account for NO_x transformations between emission and sampling. Correlations were determined using orthogonal distance regression, the straight-line fit type commonly used in this field when both *x* and *y* variables have associated measurements errors (Anderson et al., 2014; Pollack et al., 2012). The regressions were weighted by each variable's uncertainties, and the *y*-intercepts forced through zero. A detailed discussion of the straight-line fitting is provided in Text S5 (Wehr & Saleska, 2017; York et al., 2004).

3.2.1. CO/NO_x

Figure 6 shows the CO/NO_x enhancement ratios calculated from UMD flight measurements (corresponding values are listed in Table S4). CO/NO_x enhancement ratios observed during WINTER are compared with estimates from the NEI and other urban studies (Figure 6). The average CO/NO_x emission ratio observed during D.C.-Balt mass balance flights is 4.6 (95% CI: ±0.7) ppbv $ppbv^{-1}$ (individual flight day values are provided in Table S4). The average urban CO/NO_x enhancement ratio determined from C-130 measurements within the D.C.-Balt, Philadelphia, PA, and Cincinnati, OH urban plumes was 5.1 (95% CI: ±1.5) ppbv $ppbv^{-1}$. The NEI CO/NO_x is a factor of ~2.0 greater than the emission ratios calculated from both the UMD aircraft and C-130 observations.

The average CO/NO_x for the UMD aircraft flights is the average of ratios calculated for five flight days (between 13 and 25 February 2015) and ranges from 3.4 to 5.2 ppbv $ppbv^{-1}$. The C-130 CO/NO_x enhancement ratios range from 2.8 to 6.4 ppbv $ppbv^{-1}$ and were determined from measurements conducted on 3 February 2015 (D.C.-Balt and Philadelphia, PA) and 6 February 2015 (Cincinnati, OH). Similar to the large range in day-to-day CO/NO_x enhancement ratios observed during the WINTER campaign, Simon et al. (2018) also report large daily variability in CO/NO_y enhancement ratios (4.9–13.6) in D.C.-Balt from airborne observations conducted in July 2011 (DISCOVER-AQ). Emitted ratios of CO/NO_x from different combustion sources can be highly variable; for example, CO/NO_x emission ratios from gasoline on-road vehicles are 3 orders of magnitude greater than power plant emission ratios (Simon et al., 2018). With the exception of fires (agricultural, wood), the NEI predicts gasoline vehicles and nonroad mobile equipment (construction, lawn, and recreation equipment/vehicles) emit the highest CO/NO_x ratios relative to other combustion sources (Simon et al., 2018; Wallace et al., 2012). These relatively high NEI-predicted CO/NO_x ratios are supported by in-use vehicle fleet CO/NO_x ratio measurements in Chicago (9.8; Fall 2014; Bishop et al., 2016), Tulsa (11.5; Fall 2015; Bishop & Stedman, 2016), and Los Angeles (7.7–10.7; Summer 2010; Bishop et al., 2012; Fujita et al., 2012). It is possible that the variability in daily WINTER CO/NO_x enhancement ratios is a result of varying contributions from mainly point and nonpoint sources (Table 1; e.g., energy generating facilities and industrial processes) that emit at characteristically lower CO/NO_x ratios, mixing with dominant mobile emissions in the D.C.-Balt plume.

An average enhancement ratio of 11.1 mol CO/mol NO_y was estimated from measurements during DISCOVER-AQ flights in July 2011 around Baltimore, MD (Anderson et al., 2014; Anderson, 2016). Studies in Los Angeles during CalNex 2010 (Brioude et al., 2013; Pollack et al., 2012) and Houston during TexAQS 2006 (ratio of average observed CO and NO_y mixing ratios; Yu et al., 2012) have reported CO/NO_y emission ratios ranging from 7.4 to 9.1 mol CO/mol NO_y. A possible explanation for the lower CO/NO_x observed during WINTER is that the DISCOVER-AQ, CalNex, and TexAQS campaigns were conducted between late spring and early fall. Ambient surface temperatures during the WINTER campaign were much lower and were frequently below 0 °C. Roadside morning rush hour (6–9 A.M.) measurements of CO and NO_x in Baltimore, MD in 2015 and 2016 show a similar trend, where wintertime CO/NO_x ratios are much lower when ambient temperatures are low (Figure S8). Details of these observations will be discussed in a forthcoming paper. It is possible that seasonal differences in CO/NO_x ratios (Figure S8) could result from seasonal differences in vehicle fleet composition, that is, more reliable, better maintained vehicles being used more frequently in winter relative to summer. However, Anderson (2016) shows that airborne measurements of CO/NO_y ratios in

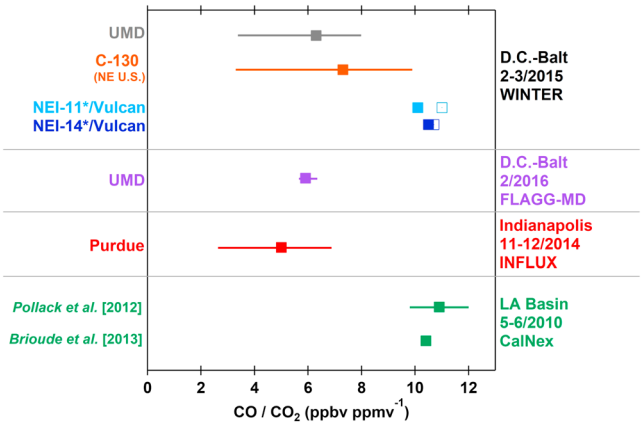

Figure 7. CO/CO_2 enhancement ratios calculated from the University of Maryland and C-130 observations during Wintertime INvestigation of Transport, Emissions, and Reactivity (WINTER). The bars indicate ranges of observed CO/CO_2 enhancement ratios. WINTER CO/CO_2 enhancement ratios are compared with CO/CO_2 estimates from the National Emissions Inventory (NEI) CO/Vulcan CO_2 and other urban studies. The unfilled and filled NEI markers indicate original NEI emissions and NEI emissions forward-projected to 2015, respectively.

Baltimore in July 2011 (DISCOVER-AQ) increased by more than a factor of 2 as the potential temperature increased from 296 to 309 K. More study is required to characterize this apparent CO/NO_x temperature dependence.

Brioude et al. (2013) report a 9% decrease in CO/NO_y emission ratio from 2002 to 2010 in the Los Angeles Basin. Miyazaki et al. (2017) report a ~30% decrease in U.S. NO_x emissions from 2005 to 2014, and Hassler et al. (2016) show that U.S. CO emissions have been decreasing at a faster rate than NO_x emissions since the 1970s. The lower CO/NO_x observed during WINTER could result from a combination of the temperature-dependence of CO/NO_x emission ratios (Figure S8) and faster mobile source CO reduction relative to NO_x (Hassler et al., 2016).

The temperature dependence of CO/NO_x enhancement ratios and relative rates of CO and NO_x emission reductions may partially explain why CO/NO_x during WINTER is lower than reported in other urban studies. However, it cannot explain the difference between WINTER observations downwind of D.C.-Balt and NEI CO/NO_x estimates in winter months. The NEI used in this study accounts for all sources of CO (Table 1) at monthly resolution. Anderson et al. (2014) note an increase in CO/NO_x ratios at midday due to the influence of BVOC oxidation; we do not expect significant impacts of BVOC oxidation on WINTER D.C.-Balt CO/NO_x ratios because most vegetation in wintertime is dormant, and OH concentrations are lower than in summer. Calculated production of CO via BVOC oxidation accounts for less than 1% of NEI D.C.-Balt CO emissions for the WINTER study months (Table 1). Another possible explanation of the lower WINTER CO/NO_x ratios is that NO_x and NO_y are relatively long-lived in winter relative to summer, but CO production via BVOC oxidation is slower in winter than summer. Combined, these effects would result in lower wintertime CO/NO_x ratios relative to summer. However, the consistency of WINTER NO_x/CO_2 enhancement ratios with those reported from other urban summertime studies (section 3.2.3) suggests that this artifact is not important, at least for NO_x.

Because inventory and observed NO_x emissions are consistent for D.C.-Balt during WINTER, and mobile emissions are the dominant source of CO (Table 1), and there is an apparent temperature dependence in mobile CO/NO_x (Figure S8), it is possible the EPA MOVES model, which provides the mobile source emissions for the NEI (EPA, 2015c), is not accurately representing wintertime mobile CO emissions. Wallace et al. (2012) show that MOVES "off-network" mobile emissions (engine starts, extended idling) account for 65% and 23% of CO and NO_x emissions, respectively, for the Boise, ID area, and are a factor of 2 larger than MOVES mobile running emissions (i.e., not off-network). Wallace et al. (2012)'s wintertime observations of CO/NO_x ratios (4.6) near a busy roadway are in agreement with our WINTER observations in D.C.-Balt (4.6 ± 0.8) and are roughly a factor of 2 lower than predicted by MOVES. The MOVES model's possible overestimation of off-network CO/NO_x enhancement ratios or off-network contributions during wintertime could be another possible source of the WINTER observations-NEI CO discrepancy (Wallace et al., 2012).

3.2.2. CO/CO_2

Figure 7 shows the averaged CO/CO_2 enhancement ratios observed during the UMD transects downwind of D.C.-Balt (values for individual flight days are provided in Table S5). The NEI CO/CO_2 ratio (10.1 ppbv $ppmv^{-1}$) is approximately 1.5 times greater than the observation-derived CO/CO_2 ratios from the UMD mass balance flights (6.3 [95% CI: ±1.8] ppbv $ppmv^{-1}$).

Figure 7 shows that the CO/CO_2 enhancement ratio, 7.3 (95% CI: ±2.6) ppbv $ppmv^{-1}$ from the C-130 flight downwind of D.C.-Balt, Philadelphia, and Cincinnati, is consistent with the five UMD flights around D.C.-Balt at the 95% CI. Again, the large range in UMD and C-130 CO/CO_2 (and CO/NO_x) enhancement ratios might indicate large variability in enhancement ratios in wintertime, likely due to variability in CO. Large variability in NO_x/CO_2 emissions was not observed during the WINTER campaign (section 3.2.3 below). In addition to interday CO/CO_2 enhancement ratio variability, C-130 measurements within the Philadelphia, PA urban plume on 3 February 2015 (Figure 3a) reveal intraday variability. The C-130 sampled the Philadelphia

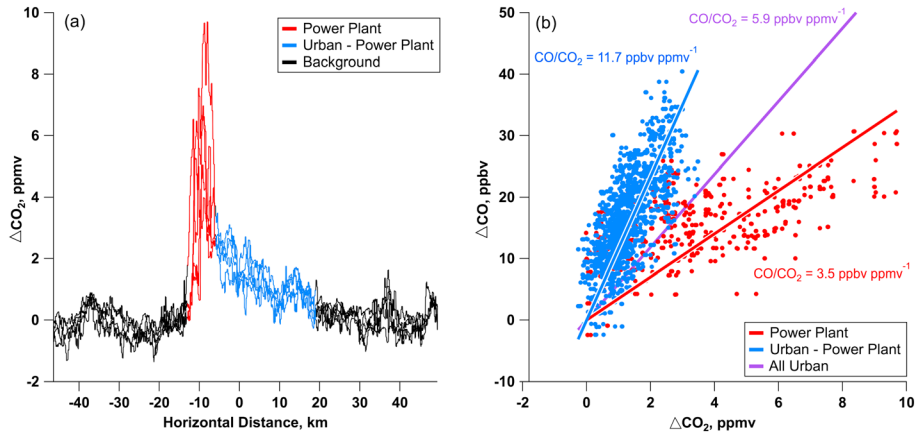

Figure 8. (a) CO_2 enhancements calculated downwind of Indianapolis on 14 November 2014. Emissions from the power plant (red) and remaining urban plume (blue) are distinguished from the background (black). (b) CO/CO_2 enhancement ratios corresponding to power plant (red) and remaining urban (blue) emissions. The CO/CO_2 enhancement ratios for the entire urban area are indicated by the purple line.

plume at two altitudes, 250 and 75 m above sea level, separated in time by 1 hr. The CO/CO_2 enhancement ratio observed along the second downwind transect was ~25% lower relative to the first. Explanations for the intraday and interday CO/CO_2 enhancement ratio variability are explored below.

Figure 7 also shows CO/CO_2 enhancement ratios observed by the UMD aircraft in D.C.-Balt for the year after WINTER (February 2016), as well as CO/CO_2 enhancement ratios observed by the Purdue aircraft during a 3-week observations period in Indianapolis in November–December 2014 (Heimburger et al., 2017). This is a useful comparison, since mobile sources (on-road + nonroad) account for 77% (Table 1) and 93% of D.C.-Balt and Indianapolis CO emissions during the measurement months (EPA, 2016a), respectively, and we expect the D.C.-Balt and Indianapolis mobile fleets to be comparable. As indicated by Figure 7, a large range in individual CO/CO_2 enhancement ratios was observed in D.C.-Balt during WINTER and in Indianapolis in 2014. However, the average CO/CO_2 enhancements ratios in D.C.-Balt in 2015 and 2016 and in Indianapolis in 2014 are similar (6.3, 5.9, and 5.0 ppbv $ppmv^{-1}$, respectively). Air parcel transport times between emission and sampling are shorter in Indianapolis due to the city's smaller size and a less-restricted flight area. Because of this, unique emission ratios from specific sources can be distinguishable if transport times are short, which could minimize mixing of emissions from different sectors. Thus, observations in Indianapolis may provide information about sector-specific CO/CO_2 emission ratios and explanations for CO/CO_2 enhancement ratio variability.

Figure 8 provides a possible explanation for the observed variability in CO/CO_2 emission ratios. Figure 8a shows the background-subtracted CO_2 enhancement observed downwind of Indianapolis on 14 November 2014. CO_2 mixing ratios are greatest downwind of the city's main power plant, which was coal-fired at the time, while a smaller CO_2 enhancement is observed downwind of the rest of the city. Figure 8b shows three CO/CO_2 correlation slopes for the power plant (3.5 ppbv $ppmv^{-1}$), urban area minus the power plant (11.7 ppbv $ppmv^{-1}$), and for the entire urban area (5.9 ppbv $ppmv^{-1}$). Distinct sector correlation slopes, such as the ones shown in Figure 8b, were observed on some of the February 2014 flight days in Indianapolis. The presence of observationally distinct sector-specific CO/CO_2 correlations is likely dependent on wind speed and the distance of the downwind flight tracks from the emission source (s). Although there are major power plants in the D.C.-Balt area, distinct sector correlations were not observed in D.C.-Balt, probably because D.C.-Balt is larger and more complex than Indianapolis in terms of number and type of point sources and transport times are longer, allowing for mixing of sector-specific emission ratios. The "urban minus power plant" CO/CO_2 emission ratio of 11.7 ppbv $ppmv^{-1}$, mainly a result of mobile source emissions, is closer to the emission ratios reported during CalNex 2010 and estimated from inventories (NEI CO/Vulcan CO_2) for D.C.-Balt during WINTER. The mixing of mobile emissions from other sources in the urban environment as evidenced by the CO/NO_x enhancement ratios is further supported by the variability observed in CO/CO_2

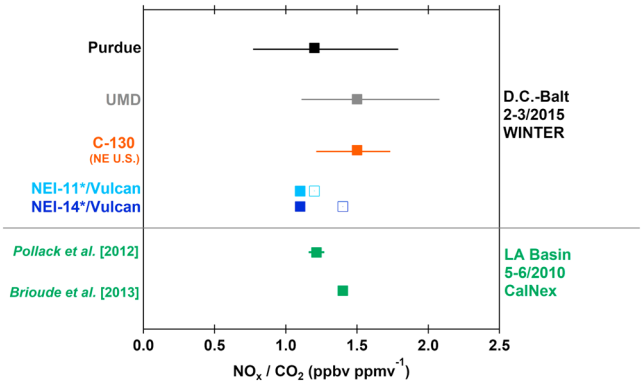

Figure 9. NO_x/CO_2 enhancement ratios calculated from University of Maryland, Purdue, and C-130 observations. The bars indicate ranges of observed CO/CO_2 enhancement ratios. Observed enhancement ratios during Wintertime INvestigation of Transport, Emissions, and Reactivity are compared with estimates from the National Emissions Inventory (NEI) and other urban studies. The unfilled and filled NEI markers indicate original NEI emissions and NEI emissions forward-projected to 2015, respectively.

enhancement ratios. It is thus likely that observed wintertime CO/CO_2 enhancement ratio variability within a city depends on the presence, operational state, and fueling of power plants, which can have temporally variable CO emissions and much lower CO/CO_2 emission ratios (Nicks Jr et al., 2003; Peischl et al., 2010). Nicks Jr et al. (2003) reported observing an eightfold change in power plant CO emissions over the course of 1 hr. Few power plants emit substantial amounts of CO; the Chalk Point power plant in Maryland (Figure 5b) is an example of low CO/CO_2. Because the Indianapolis power plant is located within the city, it is possible the CO/CO_2 correlation in Figure 8b is due to spatial collocation of the Indianapolis power plant CO_2 emissions and mobile CO emissions. Diesel combustion (nonroad equipment, generators, and vehicles) produces emissions with characteristically low CO/CO_2 ratios as well and could be partially responsible for the relatively low and variable CO/CO_2 ratios observed in D.C.-Balt and Indianapolis (Figure 7; Heidari & Marr, 2015).

3.2.3. NO_x/CO_2

Figure 9 shows NO_x/CO_2 enhancement ratios for the Purdue and UMD flights (corresponding values are listed in Table S6). NO_x/CO_2 measured by the C-130 within urban plumes along the northeast United States, 1.5 (95% CI: ±0.2) ppbv $ppmv^{-1}$, are consistent with the average university aircraft observations, 1.4 (95% CI: ±0.4) ppbv $ppmv^{-1}$. NO_x/CO_2 observed during WINTER are similar to emission ratios reported during CalNex 2010 (1.16–1.4 ppbv $ppmv^{-1}$; Brioude et al., 2013; Pollack et al., 2012) and to the ratio of NEI-11 and NEI-14 NO_x to scaled Vulcan CO_2 (section 2.8), 1.1 for both NEI versions. NO_x/CO_2 enhancement ratios measured on 19 February 2015 from the Chalk Point Generating Facility were estimated to be 1.8 (±0.7) ppbv $ppmv^{-1}$, while the emission ratio reported by CEMS was 1.83 (1σ: ±0.07) ppbv $ppmv^{-1}$. Unlike enhancement ratios with CO, observed WINTER NO_x/CO_2 enhancement ratios are consistent with the NEI/Vulcan NO_x/CO_2 emission ratios.

Mobile sources in D.C.-Balt also dominate the area's NO_x emissions (Table 1). Considering the consistency between the NEI and observed NO_x emission rates and NO_x/CO_2 enhancement ratios, our observations could indicate that MOVES captures the area's mobile NO_x emissions reasonably well. However, studies have shown that MOVES NO_x emissions are very sensitive to input data, such as the distribution of vehicle types, vehicle speeds, and vehicle miles traveled (de Foy, 2018; Fujita et al., 2012). Diesel/heavy duty vehicles have comparatively higher NO_x emissions relative to gasoline/light-duty vehicles (Fujita et al., 2012; Hassler et al., 2016). NO_x emissions predicted by the MOVES model should still be assessed for other cities or regions.

3.2.4. Criteria Pollutant Emission Rate Method Comparison

Here we conduct a proof of concept exercise to demonstrate that criterion pollutant/CO_2 enhancement ratios (X/CO_2, e.g., NO_x/CO_2 and CO/CO_2) can be multiplied by high-resolution CO_2 inventories to provide criteria pollutant emission rates for cities. We show that NO_x and CO emission rates from $X/CO_2 \times$ Vulcan CO_2 are consistent with the D.C.-Balt NO_x and CO emission rates calculated using the mass balance approach (section 2.7). We conduct a similar exercise with the Indianapolis Winter 2014 CO/CO_2 enhancement ratio reported in this study and the Hestia Indianapolis CO_2 emission rate and see agreement with the mass balance CO emission rate reported from the area by Heimburger et al. (2017). The results of the exercise are provided in Table 2.

It is not surprising that the enhancement ratio-derived emission rates are in better agreement with the mass balance-derived emission rates than the NEI. Both approaches use the same background-subtracted urban NO_x and CO enhancements. However, the agreement between the two methods also hinges on the accuracy of the CO_2 inventory. Development of high-resolution and national-scale CO_2 inventories can be done relatively reliably. If robust NO_x/CO_2 and CO/CO_2 emission factors are determined for each contributing sector, the fuel- and activity-based Hestia CO_2 inventory can eventually be used to produce nationwide NO_x and CO inventories independent of the NEI. We emphasize that sector-specific (not city-wide) emission factors would need to be used to convert the high-resolution CO_2 inventories for other cities.

Table 2
Criteria Pollutant Emission Rate Method Comparison

City/campaign or date	X/CO_2 enhancement ratio [ppbv ppmv^{-1}]	CO_2 inventory: Emission rate [mol s^{-1}]	X/CO_2 × CO_2 inventory [mol s^{-1}]	Mass balance emission rate [mol s^{-1}]	NEI-11[a] emission rate [mol s^{-1}]
Species	CO/CO_2	CO_2	CO	CO	CO
D.C.-Balt WINTER 2015	6.3 (±0.4)	Vulcan[b] 1.03×10^5	650 (±185)	540 (±470)	1,100
Indianapolis November–December 2014	5.0 (±1.0)	Hestia: 1.51×10^4	75 (±15)	108 (±17)[c]	150
Species	NO_x/CO_2	CO_2	NO_x	NO_x	NO_x
D.C.-Balt WINTER 2015	1.4 (±0.4)	Vulcan[†]: 1.03×10^5	145 (±40)	130 (±70)	115

Note. All numbers in parentheses correspond to the 95% CI.
[a]The NEI-11 forward-projected to 2015 (Text S4). [b]The Vulcan 2002 CO_2 inventory estimate has been scaled by D.C.-Balt population growth (18%) from 2002 to 2015 (Text S4). [c]Heimburger et al. (2017).

This analysis also highlights a need for an updated nationwide CO_2 inventory. As more high-resolution fuel-use-based CO_2 emissions inventories are available for major U.S. cities (Gurney et al., 2012; Newman et al., 2016; Patarasuk et al., 2016), reporting observed city-scale emission ratios of criteria pollutants, like NO_x and CO, relative to CO_2 could be useful for evaluating observation-based criteria pollutant inventories (Hsu et al., 2010; Warneke et al., 2007). Validation of such an inventory can only be done reliably in the winter, when an inactive biosphere makes CO_2 a more conserved tracer.

4. Conclusions

Measurements conducted during mass balance flights around D.C.-Balt during the WINTER campaign were used to quantify city-wide emission rates of NO_x and CO. D.C.-Balt top-down NO_x emission rate estimates were 130 mol s^{-1} on average in February and March 2015, consistent with the NEI within the mass balance measurement uncertainty. The average CO emission rate determined from five mass balance estimates was 540 mol s^{-1}, approximately a factor of 2 lower than the emission rate reported by the NEI. The WINTER D.C.-Balt NO_x/CO_2 enhancement ratios are similar compared to those reported from other cities around the United States. The WINTER CO/NO_x and CO/CO_2 enhancement ratios were smaller than reported by other urban studies and have large ranges estimated from the research flights.

These relatively small WINTER CO/NO_x and CO/CO_2 enhancement ratios could result from continuing reductions in mobile CO emissions, as reported by Hassler et al. (2016). There is also evidence of a temperature dependence of CO/NO_x enhancement ratios from airborne observations in D.C.-Balt (Anderson, 2016). Observations of wintertime roadway emissions indicate that the MOVES model overestimates off-network CO/NO_x enhancement ratios or relative contributions and could be a significant source of uncertainty considering that on-road mobile emissions are the dominant source of CO and NO_x emissions in urban areas (Wallace et al., 2012). Several studies have also noted the uncertainty in NEI nonroad emissions, the second largest source of CO and NO_x emissions, since many types of vehicles/equipment fall into the category (e.g., construction, agriculture, lawn/garden, and recreation vehicles and equipment) and have unique emission profiles (Dallmann & Harley, 2010; Heidari & Marr, 2015). Together, the observations-NEI agreement in winter NO_x emissions, but discrepancy in CO emissions, and the apparent temperature dependence of CO/NO_x enhancement ratios may indicate that on-road and nonroad emissions need to be assessed as a function of temperature and operating conditions and mobile models updated.

The variability in WINTER CO/NO_x and CO/CO_2 enhancement ratios may be a result of the dominant mobile emissions in D.C.-Balt being diluted to varying degrees by emissions from other source sectors. We show an example of this using the relatively simple urban environment of Indianapolis on a day when unique CO/CO_2 enhancement ratios were clearly distinguishable in the urban plume. Power plant emissions could be responsible for the low wintertime CO/CO_2 enhancement ratios observed during WINTER in D.C.-Balt, and in Indianapolis relative to the enhancement ratios expected from purely mobile emissions. Future studies should consider the location of power plants (within or outside of the urban area) and their potential impact when reporting urban CO/CO_2 enhancement ratios. We do note as well that diesel combustion can also produce emissions with characteristically low CO/CO_2.

The NEI has been evaluated for decades with top-down NO_x and CO estimates from entire cities or specific sectors. While the NEI represents winter D.C.-Balt NO_x emissions relatively well, our observations suggest the NEI significantly overestimates wintertime D.C.-Balt and Indianapolis CO emissions. Given that mobile (on-road + nonroad) emissions are responsible for most U.S. anthropogenic CO emissions, it is likely that improvements to the MOVES model are necessary to accurately represent CO emissions in D.C.-Balt and Indianapolis and, presumably, nationally. Many studies suggesting mobile emissions as being overestimated by the NEI speak to the complexity of accurately modeling emissions from a continuously changing vehicle fleet operating at different conditions under continuously updated vehicle emissions standards (Canty et al., 2015; Parrish, 2006; Travis et al., 2016). However, even if MOVES perfectly describes emissions for every type of vehicle, it could generate incorrect emissions if input data, such as fleet age, composition, and driving patterns, are changing (de Foy, 2018).

Efforts are being directed toward applying Hestia, an urban-scale CO_2 inventory, to more cities, as well as a 1-km^2 version of the national-scale Vulcan CO_2 inventory. Hestia CO_2 emissions are available for Baltimore and Indianapolis (Gurney et al., 2012), used in our analysis, as well as Salt Lake City (Patarasuk et al., 2006), and Los Angeles (Newman et al., 2016). If robust NO_x/CO_2 and CO/CO_2 emission factors are determined for contributing sectors, the fuel-use-based Hestia CO_2 inventory can eventually be used to produce NO_x and CO inventories independent of the NEI. This would then result in much more reliable NO_x and CO inventories, if the inventory was validated during winter when CO_2 is a conserved tracer, and as long as emission factors were regularly updated. Through a proof of concept exercise, we show agreement between our mass balance city-wide emission rate determinations and emission rates derived from emission ratios and inventory CO_2 emission rates for Indianapolis and D.C.-Balt. City-wide enhancement ratios such as the ones reported in this study could be used to complement the development of such criteria pollutant emission inventories.

Wintertime INvestigation of Transport, Emissions, and Reactivity is the first major airborne study designed specifically to investigate urban cold season emissions. An advantage of conducting measurements in wintertime is that reduced BVOC emissions, biosphere CO_2 exchange, and slower photochemical oxidation rates make quantifying absolute urban emissions less complicated. However, our WINTER measurements in D.C.-Balt reveal lower and variable CO/CO_2 and CO/NO_x enhancement ratios relative to summertime urban studies around the United States. Campaigns that prioritize less-frequently studied seasons would address this measurement gap.

Acknowledgments

We are grateful for help with the design, installation, and maintenance of the ALAR instrument package we received from Purdue University's Jonathan Amy Facility for Chemical Instrumentation. We acknowledge support for this research from James Whetstone and NIST. The UMD and Purdue flight experiments and analysis were supported by NIST Award 70NANB14H333 and 70NANB14H332, respectively. The WINTER campaign was supported through NSF AGS-1360745. All airborne data collected during the WINTER campaign by the Purdue, UMD, and C-130 aircraft are available on the WINTER Data Archive at EOL: http://data.eol.ucar.edu/master_list/?project=WINTER. Vulcan 2002 CO_2 data is available at http://vulcan.project.asu.edu/research.php. UMD acknowledges support from MDE for RAMMPP. Funding for D. L. Fibiger was supported by the NSF award 1433358.

References

Acevedo, O. C., & Fitzjarrald, D. R. (2001). The early evening surface-layer transition: Temporal and spatial variability. *Journal of the Atmospheric Sciences*, *58*(17), 2650–2667. https://doi.org/10.1175/1520-0469(2001)058<2650:teeslt>2.0.co;2

Ahmadov, R., McKeen, S., Trainer, M., Banta, R., Brewer, A., Brown, S., et al. (2015). Understanding high wintertime ozone pollution events in an oil- and natural gas-producing region of the western US. *Atmospheric Chemistry and Physics*, *15*(1), 411–429. https://doi.org/10.5194/acp-15-411-2015

Anderson, D. C., Loughner, C. P., Diskin, G., Weinheimer, A., Canty, T. P., Salawitch, R. J., et al. (2014). Measured and modeled CO and NOy in DISCOVER-AQ: An evaluation of emissions and chemistry over the eastern US. *Atmospheric Environment*, *96*, 78–87. https://doi.org/10.1016/j.atmosenv.2014.07.004

Anderson, D. C. (2016). *Photochemistry and transport of tropospheric ozone and its precursors in urban and remote environments*. College Park: University of Maryland.

Beirle, S., Boersma, K. F., Platt, U., Lawrence, M. G., & Wagner, T. (2011). Megacity emissions and lifetimes of nitrogen oxides probed from space. *Science*, *333*(6050), 1737–1739. https://doi.org/10.1126/science.1207824

Berg, L., & Allwine, K. J. (2006). *An analysis of wintertime winds in Washington, DC, edited, PNNL–15799*. Richland, Washington: Pacific Northwest National Laboratory.

Bishop, G. A., Schuchmann, B. G., Stedman, D. H., & Lawson, D. R. (2012). Multispecies remote sensing measurements of vehicle emissions on Sherman Way in Van Nuys, California. *Journal of the Air & Waste Management Association*, *62*(10), 1127–1133. https://doi.org/10.1080/10962247.2012.699015

Bishop, G. A., & Stedman, D. H. (2008). A decade of on-road emissions measurements. *Environmental Science & Technology*, *42*(5), 1651–1656. https://doi.org/10.1021/es702413b

Bishop, G. A., & Stedman, D. H. (2015). Reactive nitrogen species emission trends in three light-/medium-duty United States fleets. *Environmental Science & Technology*, *49*(18), 11,234–11,240. https://doi.org/10.1021/acs.est.5b02392

Bishop, G. A., & Stedman, D. H. (2016). On-road remote sensing of automobile emissions in the Tulsa area: Fall 2015, final report prepared for CRC, June 2016.

Bishop, G. A., Stedman, D. H., Burgard, D. A., & Atkinson, O. (2016). High-mileage light-duty fleet vehicle emissions: Their potentially overlooked importance. *Environmental Science & Technology*, *50*(10), 5405–5411. https://doi.org/10.1021/acs.est.6b00717

Bonin, T. A., Carroll, B. J., Hardesty, R. M., Brewer, W. A., Hajny, K., Salmon, O. E., & Shepson, P. B. (2018). Doppler Lidar observations of the mixing height in Indianapolis using an automated composite fuzzy logic approach. *Journal of Atmospheric and Oceanic Technology*, *35*(3), 473–490. https://doi.org/10.1175/jtech-d-17-0159.1

Brent, L. C., Thorn, W. J., Gupta, M., Leen, J. B., Stehr, J. W., He, H., et al. (2015). Evaluation of the use of a commercially available cavity ringdown absorption spectrometer for measuring NO2 in flight, and observations over the mid-Atlantic states, during DISCOVER-AQ. *Journal of Atmospheric Chemistry*, *72*(3-4), 503–521. https://doi.org/10.1007/s10874-013-9265-6

Brioude, J., Angevine, W. M., Ahmadov, R., Kim, S. W., Evan, S., McKeen, S. A., et al. (2013). Top-down estimate of surface flux in the Los Angeles Basin using a mesoscale inverse modeling technique: Assessing anthropogenic emissions of CO, NOx and CO_2 and their impacts. *Atmospheric Chemistry and Physics*, *13*(7), 3661–3677. https://doi.org/10.5194/acp-13-3661-2013

Cambaliza, M. O. L., Shepson, P. B., Bogner, J., Caulton, D. R., Stirm, B. H., Sweeney, C., et al. (2015). Quantification and source apportionment of the methane emission flux from the city of Indianapolis. *Elementa*, *3*(1), 000037. https://doi.org/10.12952/journal.elementa.000037

Cambaliza, M. O. L., Shepson, P. B., Caulton, D. R., Stirm, B. H., Samarov, D., Gurney, K. R., et al. (2014). Assessment of uncertainties of an aircraft-based mass balance approach for quantifying urban greenhouse gas emissions. *Atmospheric Chemistry and Physics*, *14*(17), 9029–9050. https://doi.org/10.5194/acp-14-9029-2014

Canty, T. P., Hembeck, L., Vinciguerra, T. P., Anderson, D. C., Goldberg, D. L., Carpenter, S. F., et al. (2015). Ozone and NOx chemistry in the eastern US: Evaluation of CMAQ/CB05 with satellite (OMI) data. *Atmospheric Chemistry and Physics*, *15*(19), 10,965–10,982. https://doi.org/10.5194/acp-15-10965-2015

Castellanos, P., Marufu, L. T., Doddridge, B. G., Taubman, B. F., Schwab, J. J., Hains, J. C., et al. (2011). Ozone, oxides of nitrogen, and carbon monoxide during pollution events over the eastern United States: An evaluation of emissions and vertical mixing. *Journal of Geophysical Research*, *116*, D16307. https://doi.org/10.1029/2010jd014540

Chou, C. C. K., Tsai, C.-Y., Shiu, C.-J., Liu, S. C., & Zhu, T. (2009). Measurement of NOy during campaign of air quality research in Beijing 2006 (CAREBeijing-2006): Implications for the ozone production efficiency of NOx. *Journal of Geophysical Research*, *114*, D00G01. https://doi.org/10.1029/2008jd010446

Cobb, N., & Etzel, R. A. (1991). Unintentional carbon monoxide—Related deaths in the United States, 1979 through 1988. *JAMA*, *266*(5), 659–663. https://doi.org/10.1001/jama.1991.03470050059023

Dallmann, T. R., & Harley, R. A. (2010). Evaluation of mobile source emission trends in the United States. *Journal of Geophysical Research*, *115*, D14305. https://doi.org/10.1029/2010jd013862

Davis, K. J., Deng, A., Lauvaux, T., Miles, N. L., Richardson, S. J., Sarmiento, D. P., et al. (2017). The Indianapolis Flux Experiment (INFLUX): A test-bed for developing urban greenhouse gas emission measurements. *Elementa: Science of the Anthropocene*, *5*(0). https://doi.org/10.1525/elementa.188

de Foy, B. (2018). City-level variations in NOx emissions derived from hourly monitoring data in Chicago. *Atmospheric Environment*, *176*, 128–139. https://doi.org/10.1016/j.atmosenv.2017.12.028

EPA (2004). The Clean Air Act [as amended through P.L. 108–201, February 24, 2004], EPA, Washington, D.C.

EPA (2014a). Technical support document (TSD) preparation of emissions inventories for the version 6.0, 2011 emissions modeling platform. Retrieved June 2015 from http://www.epa.gov/ttn/chief/emch/2011v6/outreach/2011v6_2018base_EmisMod_TSD_26feb2014.pdf

EPA (2014b). Meteorology technical support document—Meteorological model performance for annual 2011 WRF v3.4 SIMULATION. Retrieved June 2015 from http://www.epa.gov/ttn/scram/reports/MET_TSD_2011_final_11-26-14.pdf

EPA (2015a). Chapter 2 selective catalytic reduction, June 2015, EPA, Research Triangle Park, NC.

EPA (2015b). 2011 National Emission Inventory, version 2 technical support document, August 2015, EPA, Washington, D.C.

EPA (2015c). Technical support document (TSD) preparation of emissions inventories for the version 6.2, 2011 Emissions modeling platform, EPA, Washington, D.C.

EPA (2016a). Approved air quality implementation plans, https://www.epa.gov/air-quality-implementation-plans/approved-air-quality-implementation-plans, EPA, Washington, D.C.

EPA (2016b). 2014 National Emission Inventory, version 1 technical support document, December 2016, EPA, Washington, D.C.

Fuchs, H., Dubé, W. P., Lerner, B. M., Wagner, N. L., Williams, E. J., & Brown, S. S. (2009). A sensitive and versatile detector for atmospheric NO2 and NOX based on blue diode laser cavity ring-down spectroscopy. *Environmental Science & Technology*, *43*(20), 7831–7836. https://doi.org/10.1021/es902067h

Fujita, E. M., Campbell, D. E., Zielinska, B., Chow, J. C., Lindhjem, C. E., DenBleyker, A., et al. (2012). Comparison of the MOVES2010a, MOBILE6.2, and EMFAC2007 MOBILE source emission models with on-road traffic tunnel and remote sensing measurements. *Journal of the Air & Waste Management Association*, *62*(10), 1134–1149. https://doi.org/10.1080/10962247.2012.699016

Garman, K., Hill, K., Wyss, P., Carlsen, M., Zimmerman, J., Stirm, B., et al. (2006). An airborne and wind tunnel evaluation of a wind turbulence measurement system for aircraft-based flux measurements. *Journal of Atmospheric and Oceanic Technology*, *23*(12), 1696–1708. https://doi.org/10.1175/JTECH1940.1

Gioli, B., Carfora, M. F., Magliulo, V., Metallo, M. C., Poli, A. A., Toscano, P., & Miglietta, F. (2014). Aircraft mass budgeting to measure CO2 emissions of Rome, Italy. *Environmental Monitoring and Assessment*, *186*(4), 2053–2066. https://doi.org/10.1007/s10661-013-3517-4

Goldberg, D. L., Vinciguerra, T. P., Anderson, D. C., Hembeck, L., Canty, T. P., Ehrman, S. H., et al. (2016). CAMx ozone source attribution in the eastern United States using guidance from observations during DISCOVER-AQ Maryland. *Geophysical Research Letters*, *43*, 2249–2258. https://doi.org/10.1002/2015GL067332

Goldberg, D. L., Vinciguerra, T. P., Hosley, K. M., Loughner, C. P., Canty, T. P., Salawitch, R. J., & Dickerson, R. R. (2015). Evidence for an increase in the ozone photochemical lifetime in the eastern United States using a regional air quality model. *Journal of Geophysical Research: Atmospheres*, *120*, 12,778–12,793. https://doi.org/10.1002/2015JD023930

Gurney, K. R., Mendoza, D. L., Zhou, Y., Fischer, M. L., Miller, C. C., Geethakumar, S., & de la Rue du Can, S. (2009). High resolution fossil fuel combustion CO2 emission fluxes for the United States. *Environmental Science & Technology*, *43*(14), 5535–5541. https://doi.org/10.1021/es900806c

Gurney, K. R., Razlivanov, I., Song, Y., Zhou, Y., Benes, B., & Abdul-Massih, M. (2012). Quantification of fossil fuel CO2 emissions on the building/street scale for a large U.S. City. *Environmental Science & Technology*, *46*(21), 12,194–12,202. https://doi.org/10.1021/es3011282

Hains, J. C., Taubman, B. F., Thompson, A. M., Stehr, J. W., Marufu, L. T., Doddridge, B. G., & Dickerson, R. R. (2008). Origins of chemical pollution derived from mid-Atlantic aircraft profiles using a clustering technique. *Atmospheric Environment*, *42*(8), 1727–1741. https://doi.org/10.1016/j.atmosenv.2007.11.052

Hassler, B., McDonald, B. C., Frost, G. J., Borbon, A., Carslaw, D. C., Civerolo, K., et al. (2016). Analysis of long-term observations of NOx and CO in megacities and application to constraining emissions inventories. *Geophysical Research Letters*, *43*, 9920–9930. https://doi.org/10.1002/2016gl069894

He, H., Loughner, C. P., Stehr, J. W., Arkinson, H. L., Brent, L. C., Follette-Cook, M. B., et al. (2014). An elevated reservoir of air pollutants over the mid-Atlantic states during the 2011 DISCOVER-AQ campaign: Airborne measurements and numerical simulations. *Atmospheric Environment*, *85*, 18–30. https://doi.org/10.1016/j.atmosenv.2013.11.039

He, H., Stehr, J. W., Hains, J. C., Krask, D. J., Doddridge, B. G., Vinnikov, K. Y., et al. (2013). Trends in emissions and concentrations of air pollutants in the lower troposphere in the Baltimore/Washington airshed from 1997 to 2011. *Atmospheric Chemistry and Physics*, *13*(15), 7859–7874. https://doi.org/10.5194/acp-13-7859-2013

He, H., Vinnikov, K. Y., Li, C., Krotkov, N. A., Jongeward, A. R., Li, Z., et al. (2016). Response of SO_2 and particulate air pollution to local and regional emission controls: A case study in Maryland. *Earth's Future*, *4*(4), 94–109. https://doi.org/10.1002/2015ef000330

Heidari, B., & Marr, L. C. (2015). Real-time emissions from construction equipment compared with model predictions. *Journal of the Air & Waste Management Association*, *65*(2), 115–125. https://doi.org/10.1080/10962247.2014.978485

Heimburger, A. M., Harvey, R. M., Shepson, P. B., Stirm, B. H., Gore, C., Turnbull, J., et al. (2017). Assessing the optimized precision of the aircraft mass balance method for measurement of urban greenhouse gas emission rates through averaging. *Elementa: Science of the Anthropocene*, *5*, 26–41. https://doi.org/10.1525/elementa.134

Horowitz, L. W., Liang, J., Gardner, G. M., & Jacob, D. J. (1998). Export of reactive nitrogen from North America during summertime: Sensitivity to hydrocarbon chemistry. *Journal of Geophysical Research*, *103*(D11), 13,451–13,476. https://doi.org/10.1029/97jd03142

Houyoux, M. R., & Vukovich, J. M. (1999). Updates to the Sparse Matrix Operator Kernel Emissions (SMOKE) modeling system and integration with Models-3. *The Emission Inventory: Regional Strategies for the Future*, *1461*, 1–11.

Hsu, Y.-K., VanCuren, T., Park, S., Jakober, C., Herner, J., FitzGibbon, M., et al. (2010). Methane emissions inventory verification in southern California. *Atmospheric Environment*, *44*(1), 1–7. http://doi.org/10.1016/j.atmosenv.2009.10.002

Huang, M., Bowman, K. W., Carmichael, G. R., Chai, T., Pierce, R. B., Worden, J. R., et al. (2014). Changes in nitrogen oxides emissions in California during 2005–2010 indicated from top-down and bottom-up emission estimates. *Journal of Geophysical Research: Atmospheres*, *119*, 12,928–12,952. https://doi.org/10.1002/2014jd022268

Hudman, R. C., Jacob, D. J., Turquety, S., Leibensperger, E. M., Murray, L. T., Wu, S., et al. (2007). Surface and lightning sources of nitrogen oxides over the United States: Magnitudes, chemical evolution, and outflow. *Journal of Geophysical Research*, *112*, D12S05. https://doi.org/10.1029/2006jd007912

Hudman, R. C., Murray, L. T., Jacob, D. J., Millet, D. B., Turquety, S., Wu, S., et al. (2008). Biogenic versus anthropogenic sources of CO in the United States. *Geophysical Research Letters*, *35*, L04801. https://doi.org/10.1029/2007gl032393

Kalthoff, N., Corsmeier, U., Schmidt, K., Kottmeier, C., Fiedler, F., Habram, M., & Slemr, F. (2002). Emissions of the city of Augsburg determined using the mass balance method. *Atmospheric Environment*, *36*(Supplement 1), 19–31. https://doi.org/10.1016/S1352-2310(02)00215-7

Karion, A., Sweeney, C., Kort, E. A., Shepson, P. B., Brewer, A., Cambaliza, M., et al. (2015). Aircraft-based estimate of Total methane emissions from the Barnett shale region. *Environmental Science & Technology*, *49*(13), 8124–8131. https://doi.org/10.1021/acs.est.5b00217

Karion, A., Sweeney, C., Pétron, G., Frost, G., Michael Hardesty, R., Kofler, J., et al. (2013). Methane emissions estimate from airborne measurements over a western United States natural gas field. *Geophysical Research Letters*, *40*(16), 4393–4397. https://doi.org/10.1002/grl.50811

Kim, S. W., Heckel, A., McKeen, S. A., Frost, G. J., Hsie, E. Y., Trainer, M. K., et al. (2006). Satellite-observed U.S. power plant NOx emission reductions and their impact on air quality. *Geophysical Research Letters*, *33*, L22812. https://doi.org/10.1029/2006gl027749

Kim, S. W., McDonald, B. C., Baidar, S., Brown, S. S., Dube, B., Ferrare, R. A., et al. (2016). Modeling the weekly cycle of NOx and CO emissions and their impacts on O3 in the Los Angeles-south coast Air Basin during the CalNex 2010 field campaign. *Journal of Geophysical Research: Atmospheres*, *121*, 1340–1360. https://doi.org/10.1002/2015jd024292

Konovalov, I. B., Beekmann, M., Richter, A., Burrows, J. P., & Hilboll, A. (2010). Multi-annual changes of NO_x emissions in megacity regions: Nonlinear trend analysis of satellite measurement based estimates. *Atmospheric Chemistry and Physics*, *10*(17), 8481–8498. https://doi.org/10.5194/acp-10-8481-2010

Kota, S. H., Ying Q., & Schade G.W. (2012). MOVES vs. MOBILE6.2: Differences in emission factors and regional air quality predictions, Transportation Research Board 91st Annual Meeting (12–4438).

Kota, S. H., Zhang, H., Chen, G., Schade, G. W., & Ying, Q. (2014). Evaluation of on-road vehicle CO and NOx National Emission Inventories using an urban-scale source-oriented air quality model. *Atmospheric Environment*, *85*, 99–108. https://doi.org/10.1016/j.atmosenv.2013.11.020

Krotkov, N. A., McLinden, C. A., Li, C., Lamsal, L. N., Celarier, E. A., Marchenko, S. V., et al. (2016). Aura OMI observations of regional SO2 and NO2 pollution changes from 2005 to 2015. *Atmospheric Chemistry and Physics*, *16*(7), 4605–4629. https://doi.org/10.5194/acp-16-4605-2016

Lamsal, L. N., Martin, R. V., Donkelaar, A. v., Celarier, E. A., Bucsela, E. J., Boersma, K. F., et al. (2010). Indirect validation of tropospheric nitrogen dioxide retrieved from the OMI satellite instrument: Insight into the seasonal variation of nitrogen oxides at northern midlatitudes. *Journal of Geophysical Research*, *115*, D05302. https://doi.org/10.1029/2009JD013351

Lavoie, T. N., Shepson, P. B., Cambaliza, M. O., Stirm, B. H., Karion, A., Sweeney, C., et al. (2015). Aircraft-based measurements of point source methane emissions in the Barnett shale basin. *Environmental Science & Technology*, *49*(13), 7904–7913. https://doi.org/10.1021/acs.est.5b00410

Lavoie, T. N., Shepson, P. B., Cambaliza, M. O. L., Stirm, B. H., Conley, S., Mehrotra, S., et al. (2017). Spatiotemporal variability of methane emissions at oil and natural gas operations in the eagle Ford Basin. *Environmental Science & Technology*, *51*(14), 8001–8009. https://doi.org/10.1021/acs.est.7b00814

Leighton, P. A. (1961). *Photochemistry of air pollution*, (p. 300). New York: Academic Press.

Lothon, M., Lohou, F., Pino, D., Couvreux, F., Pardyjak, E. R., Reuder, J., et al. (2014). The BLLAST field experiment: Boundary-layer late afternoon and sunset turbulence. *Atmospheric Chemistry and Physics*, *14*(20), 10,931–10,960. https://doi.org/10.5194/acp-14-10931-2014

Marr, L. C., Moore, T. O., Klapmeyer, M. E., & Killar, M. B. (2013). Comparison of NOx fluxes measured by eddy covariance to emission inventories and land use. *Environmental Science & Technology*, *47*(4), 1800–1808. https://doi.org/10.1021/es303150y

Marufu, L. T., Taubman, B. F., Bloomer, B., Piety, C. A., Doddridge, B. G., Stehr, J. W., & Dickerson, R. R. (2004). The 2003 North American electrical blackout: An accidental experiment in atmospheric chemistry. *Geophysical Research Letters*, *31*, L13106. https://doi.org/10.1029/2004gl019771

Mays, K. L., Shepson, P. B., Stirm, B. H., Karion, A., Sweeney, C., & Gurney, K. R. (2009). Aircraft-based measurements of the carbon footprint of Indianapolis. *Environmental Science & Technology*, *43*(20), 7816–7823. https://doi.org/10.1021/es901326b

McDonald, B. C., Dallmann, T. R., Martin, E. W., & Harley, R. A. (2012). Long-term trends in nitrogen oxide emissions from motor vehicles at national, state, and air basin scales. *Journal of Geophysical Research*, *117*, D00V18. https://doi.org/10.1029/2012jd018304

Miller, S. M., Matross, D. M., Andrews, A. E., Millet, D. B., Longo, M., Gottlieb, E. W., et al. (2008). Sources of carbon monoxide and formaldehyde in North America determined from high-resolution atmospheric data. *Atmospheric Chemistry and Physics*, *8*(24), 7673–7696. https://doi.org/10.5194/acp-8-7673-2008

Miyazaki, K., Eskes, H., Sudo, K., Boersma, K. F., Bowman, K., & Kanaya, Y. (2017). Decadal changes in global surface NOx emissions from multi-constituent satellite data assimilation. *Atmospheric Chemistry and Physics*, *17*(2), 807–837. https://doi.org/10.5194/acp-2016-529

Neuman, J. A., Parrish, D. D., Trainer, M., Ryerson, T. B., Holloway, J. S., Nowak, J. B., et al. (2006). Reactive nitrogen transport and photochemistry in urban plumes over the North Atlantic Ocean. *Journal of Geophysical Research*, *111*, D23854. https://doi.org/10.1029/2005jd007010

Newman, S., Xu, X., Gurney, K. R., Hsu, Y. K., Li, K. F., Jiang, X., et al. (2016). Toward consistency between trends in bottom-up CO2 emissions and top-down atmospheric measurements in the Los Angeles megacity. *Atmospheric Chemistry and Physics*, *16*(6), 3843–3863. https://doi.org/10.5194/acp-16-3843-2016

Nicks, D. K. Jr., Holloway, J. S., Ryerson, T. B., Dissly, R. W., Parrish, D. D., Frost, G. J., et al. (2003). Fossil-fueled power plants as a source of atmospheric carbon monoxide. *Journal of Environmental Monitoring*, *5*(1), 35–39. https://doi.org/10.1039/b201486f

Nisbet, E., & Weiss, R. (2010). Top-down versus bottom-up. *Science*, *328*(5983), 1241–1243. https://doi.org/10.1126/science.1189936

O'Shea, S. J., Allen, G., Fleming, Z. L., Bauguitte, S. J. B., Percival, C. J., Gallagher, M. W., et al. (2014). Area fluxes of carbon dioxide, methane, and carbon monoxide derived from airborne measurements around Greater London: A case study during summer 2012. *Journal of Geophysical Research: Atmospheres*, *119*, 4940–4952. https://doi.org/10.1002/2013jd021269

Parrish, D. D. (2006). Critical evaluation of U.S. on-road vehicle emission inventories. *Atmospheric Environment*, *40*(13), 2288–2300. https://doi.org/10.1016/j.atmosenv.2005.11.033

Parrish, D. D., Buhr, M. P., Trainer, M., Norton, R. B., Shimshock, J. P., Fehsenfeld, F. C., et al. (1993). The total reactive oxidized nitrogen levels and the partitioning between the individual species at six rural sites in eastern North America. *Journal of Geophysical Research*, *98*(D2), 2927–2939. https://doi.org/10.1029/92jd02384

Parrish, D. D., Trainer, M., Hereid, D., Williams, E. J., Olszyna, K. J., Harley, R. A., et al. (2002). Decadal change in carbon monoxide to nitrogen oxide ratio in U.S. vehicular emissions. *Journal of Geophysical Research*, *107*(D12), 4140. https://doi.org/10.1029/2001jd000720

Patarasuk, R., Gurney, K. R., O'Keeffe, D., Song, Y., Huang, J., Rao, P., et al. (2016). Urban high-resolution fossil fuel CO2 emissions quantification and exploration of emission drivers for potential policy applications. *Urban Ecosystems*, *19*(3), 1013–1039. https://doi.org/10.1007/s11252-016-0553-1

Peischl, J., Karion, A., Sweeney, C., Kort, E. A., Smith, M. L., Brandt, A. R., et al. (2016). Quantifying atmospheric methane emissions from oil and natural gas production in the Bakken shale region of North Dakota. *Journal of Geophysical Research: Atmospheres*, *121*, 6101–6111. https://doi.org/10.1002/2015jd024631

Peischl, J., Ryerson, T. B., Aikin, K. C., de Gouw, J. A., Gilman, J. B., Holloway, J. S., et al. (2015). Quantifying atmospheric methane emissions from the Haynesville, Fayetteville, and northeastern Marcellus shale gas production regions. *Journal of Geophysical Research: Atmospheres*, *120*, 2119–2139. https://doi.org/10.1002/2014jd022697

Peischl, J., Ryerson, T. B., Holloway, J. S., Parrish, D. D., Trainer, M., Frost, G. J., et al. (2010). A top-down analysis of emissions from selected Texas power plants during TexAQS 2000 and 2006. *Journal of Geophysical Research*, D16303. https://doi.org/10.1029/2009jd013527

Pétron, G., Karion, A., Sweeney, C., Miller, B. R., Montzka, S. A., Frost, G. J., et al. (2014). A new look at methane and nonmethane hydrocarbon emissions from oil and natural gas operations in the Colorado Denver-Julesburg Basin. *Journal of Geophysical Research: Atmospheres*, *119*, 6836–6852. https://doi.org/10.1002/2013JD021272

Placet, M., Mann, C. O., Gilbert, R. O., & Niefer, M. J. (2000). Emissions of ozone precursors from stationary sources. *Atmospheric Environment*, *34*(12–14), 2183–2204. https://doi.org/10.1016/S1352-2310(99)00464-1

Pollack, I. B., Ryerson, T. B., Trainer, M., Parrish, D. D., Andrews, A. E., Atlas, E. L., et al. (2012). Airborne and ground-based observations of a weekend effect in ozone, precursors, and oxidation products in the California south coast air basin. *Journal of Geophysical Research*, *117*, D00V05. https://doi.org/10.1029/2011jd016772

Pommier, M., McLinden, C. A., & Deeter, M. (2013). Relative changes in CO emissions over megacities based on observations from space. *Geophysical Research Letters*, *40*, 3766–3771. https://doi.org/10.1002/grl.50704

Pouliot, G., Wisner, E., Mobley, D., & Hunt, W. (2012). Quantification of emission factor uncertainty. *Journal of the Air & Waste Management Association*, *62*(3), 287–298. https://doi.org/10.1080/10473289.2011.649155

Ren, X., Brune, W. H., Mao, J., Mitchell, M. J., Lesher, R. L., Simpas, J. B., et al. (2006). Behavior of OH and HO2 in the winter atmosphere in New York City. *Atmospheric Environment*, *40*, 252–263. https://doi.org/10.1016/j.atmosenv.2005.11.073

Ren, X., Hall, D. L., Vinciguerra, T., Benish, S. E., Stratton, P. R., Ahn, D., et al. (2017). Methane emissions from the Marcellus Shale in southwestern Pennsylvania and northern West Virginia based on airborne measurements. *Journal of Geophysical Research: Atmospheres*, *122*, 4639–4653. https://doi.org/10.1002/2016jd026070

Russell, A. R., Valin, L. C., & Cohen, R. C. (2012). Trends in OMI NO2 observations over the United States: Effects of emission control technology and the economic recession. *Atmospheric Chemistry and Physics*, *12*(24), 12,197–12,209. https://doi.org/10.5194/acp-12-12197-2012

Ryerson, T. B., Buhr, M. P., Frost, G. J., Goldan, P. D., Holloway, J. S., Hübler, G., et al. (1998). Emissions lifetimes and ozone formation in power plant plumes. *Journal of Geophysical Research*, *103*, 22,569–22,583. https://doi.org/10.1029/98jd01620

Salmon, O. E., Shepson, P. B., Ren, X., Marquardt Collow, A. B., Miller, M. A., Carlton, A. G., et al. (2017). Urban emissions of water vapor in winter. *Journal of Geophysical Research: Atmospheres*, *122*, 9467–9484. https://doi.org/10.1002/2016jd026074

Samet, J. M., Dominici, F., Curriero, F. C., Coursac, I., & Zeger, S. L. (2000). Fine particulate air pollution and mortality in 20 U.S. cities, 1987–1994. *New England Journal of Medicine*, *343*(24), 1742–1749. https://doi.org/10.1056/nejm200012143432401

Sickles, J. E., & Shadwick, D. S. (2007). Seasonal and regional air quality and atmospheric deposition in the eastern United States. *Journal of Geophysical Research*, *112*, D17302. https://doi.org/10.1029/2006jd008356

Simon, H., Valin, L. C., Baker, K. R., Henderson, B. H., Crawford, J. H., Pusede, S. E., et al. (2018). Characterizing CO and NOy sources and relative ambient ratios in the Baltimore area using ambient measurements and source attribution modeling. *Journal of Geophysical Research: Atmospheres*, *123*, 3304–3320. https://doi.org/10.1002/2017JD027688

Singh, H. B., Salas, L., Herlth, D., Kolyer, R., Czech, E., Avery, M., et al. (2007). Reactive nitrogen distribution and partitioning in the North American troposphere and lowermost stratosphere. *Journal of Geophysical Research*, *112*, D12S04. https://doi.org/10.1029/2006jd007664

Stavrakou, T., Müller, J. F., Boersma, K. F., De Smedt, I., & van der A, R. J. (2008). Assessing the distribution and growth rates of NOx emission sources by inverting a 10-year record of NO2 satellite columns. *Geophysical Research Letters*, *35*, L10801. https://doi.org/10.1029/2008gl033521

Stein, A. F., Draxler, R. R., Rolph, G. D., Stunder, B. J. B., Cohen, M. D., & Ngan, F. (2015). NOAA's HYSPLIT atmospheric transport and dispersion modeling system. *Bulletin of the American Meteorological Society*, *96*(12), 2059–2077, https://doi.org/10.1175/BAMS-D-14-00110.1.

Stohl, A., Trainer, M., Ryerson, T. B., Holloway, J. S., & Parrish, D. D. (2002). Export of NOy from the North American boundary layer during 1996 and 1997 North Atlantic regional experiments. *Journal of Geophysical Research*, *107*(D11), 4131. https://doi.org/10.1029/2001jd000519

Taubman, B. F., Hains, J. C., Thompson, A. M., Marufu, L. T., Doddridge, B. G., Stehr, J. W., et al. (2006). Aircraft vertical profiles of trace gas and aerosol pollution over the mid-Atlantic United States: Statistics and meteorological cluster analysis. *Journal of Geophysical Research*, *111*, D10S07. https://doi.org/10.1029/2005jd006196

Thornton, J. A., Wooldridge, P. J., Cohen, R. C., Martinez, M., Harder, H., Brune, W. H., et al. (2002). Ozone production rates as a function of NOx abundances and HOx production rates in the Nashville urban plume. *Journal of Geophysical Research*, *107*(D12), 4146. https://doi.org/10.1029/2001jd000932

Trainer, M., Ridley, B., Buhr, M., Kok, G., Walega, J., Hübler, G., et al. (1995). Regional ozone and urban plumes in the southeastern United States: Birmingham, a case study. *Journal of Geophysical Research*, *100*(D9), 18,823–18,834. https://doi.org/10.1029/95JD01641

Travis, K. R., Jacob, D. J., Fisher, J. A., Kim, P. S., Marais, E. A., Zhu, L., et al. (2016). Why do models overestimate surface ozone in the Southeast United States? *Atmospheric Chemistry and Physics*, *16*(21), 13,561–13,577. https://doi.org/10.5194/acp-16-13561-2016

U.S. Census Bureau, Population Division (2016). Annual estimates of the resident population April 1, 2010 to July 1, 2015, http://factfinder.census.gov/faces/tableservices/jsf/pages/productview.xhtml?src=bkmk, U.S. Census Bureau, Washington, D.C.

Van Dingenen, R., Dentener, F. J., Raes, F., Krol, M. C., Emberson, L., & Cofala, J. (2009). The global impact of ozone on agricultural crop yields under current and future air quality legislation. *Atmospheric Environment*, *43*(3), 604–618. http://doi.org/10.1016/j.atmosenv.2008.10.033

Vinciguerra, T., Bull, E., Canty, T., He, H., Zalewsky, E., Woodman, M., et al. (2017). Expected ozone benefits of reducing nitrogen oxide (NOx) emissions from coal-fired electricity generating units in the eastern United States. *Journal of the Air & Waste Management Association*, *67*(3), 279–291. https://doi.org/10.1080/10962247.2016.1230564

Wallace, H. W., Jobson, B. T., Erickson, M. H., McCoskey, J. K., VanReken, T. M., Lamb, B. K., et al. (2012). Comparison of wintertime CO to NOx ratios to MOVES and MOBILE6.2 on-road emissions inventories. *Atmospheric Environment*, *63*, 289–297. https://doi.org/10.1016/j.atmosenv.2012.08.062

Warneke, C., McKeen, S. A., de Gouw, J. A., Goldan, P. D., Kuster, W. C., Holloway, J. S., et al. (2007). Determination of urban volatile organic compound emission ratios and comparison with an emissions database. *Journal of Geophysical Research*, *112*, D00V17. https://doi.org/10.1029/2006jd007930

Washenfelder, R. A., Wagner, N. L., Dube, W. P., & Brown, S. S. (2011). Measurement of atmospheric ozone by cavity ring-down spectroscopy. *Environmental Science & Technology*, *45*(7), 2938–2944. https://doi.org/10.1021/es103340u

Wehr, R., & Saleska, S. R. (2017). The long-solved problem of the best-fit straight line: Application to isotopic mixing lines. *Biogeosciences*, *14*(1), 17–29. https://doi.org/10.5194/bg-14-17-2017

Wild, R. J., Edwards, P. M., Dubé, W. P., Baumann, K., Edgerton, E. S., Quinn, P. K., et al. (2014). A measurement of Total reactive nitrogen, NOy, together with NO2, NO, and O3 via cavity ring-down spectroscopy. *Environmental Science & Technology*, *48*(16), 9609–9615. https://doi.org/10.1021/es501896w

Williams, E. J., Lerner, B. M., Murphy, P. C., Herndon, S. C., & Zahniser, M. S. (2009). Emissions of NOx, SO2, CO, and HCHO from commercial marine shipping during Texas Air Quality Study (TexAQS) 2006. *Journal of Geophysical Research*, *114*, D21306. https://doi.org/10.1029/2009jd012094

Yienger, J. J., Klonecki, A. A., Levy, H., Moxim, W. J., & Carmichael, G. R. (1999). An evaluation of chemistry's role in the winter-spring ozone maximum found in the northern midlatitude free troposphere. *Journal of Geophysical Research*, *104*(D3), 3655–3667. https://doi.org/10.1029/1998jd100043

York, D., Evensen, N. M., Martı´nez, M. L., & Delgado, J. D. B. (2004). Unified equations for the slope, intercept, and standard errors of the best straight line. *American Journal of Physics*, *72*(3), 367–375. https://doi.org/10.1119/1.1632486

Yu, S., Mathur, R., Pleim, J., Pouliot, G., Wong, D., Eder, B., et al. (2012). Comparative evaluation of the impact of WRF-NMM and WRF-ARW meteorology on CMAQ simulations for O3 and related species during the 2006 TexAQS/GoMACCS campaign. *Atmospheric Pollution Research*, *3*(2), 149–162. http://doi.org/10.5094/APR.2012.015

Zhang, L., Jacob, D. J., Knipping, E. M., Kumar, N., Munger, J. W., Carouge, C. C., et al. (2012). Nitrogen deposition to the United States: Distribution, sources, and processes. *Atmospheric Chemistry and Physics*, *12*(10), 4539–4554. https://doi.org/10.5194/acp-12-4539-2012

Zhang, Y., Wang, Y., Chen, G., Smeltzer, C., Crawford, J., Olson, J., et al. (2016). Large vertical gradient of reactive nitrogen oxides in the boundary layer: Modeling analysis of DISCOVER-AQ 2011 observations. *Journal of Geophysical Research: Atmospheres*, *121*, 1922–1934. https://doi.org/10.1002/2015jd024203